

ABSTRACT OF THE THESIS OF

Pei Lun Zhang for the degree of Master of Science in Chemical Engineering presented on November 21, 2018.

Title: Dechlorination of Chlorinated Phenols in Microscale Based Reactor; Mathematical Model, and Numerical Simulation.

Abstract approved _____

Goran N. Jovanovic

The micro-based reactor can be considered as two phases: the main fluid and the gel phase. When the reactants p-chlorophenol enters reactor, diffuses from the main fluid to the gel phase. The diffusion and convection of p-chlorophenol happen in the main fluid. However, there is no convection in the gel phase because the gel phase is stationary. In addition, the gel phase is made by alginate solution containing solid catalyst Fe/Pt where the reaction takes place.

In the mathematical model, it was crucial to represent all elementary reactions steps with the first order kinetics expressions, including the elements of the catalyst surface as 'reaction species'. Therefore, I developed the kinetic expression for the net rate of change of each species participating in the elementary reaction steps, designed the mass balance equations for each species participating in the chemical reaction process, and simplified the equations by using acceptable and reasonable knowledge in molecular analysis, chemical potential, chemical kinetics and phase equilibrium.

The mathematical model is built up to express the chemical kinetics for every species in the reactor, which can rightly describe the process of chemical kinetics and the species transfer. Additionally, the mathematical model involves the mass transfer for every species in the reactor. For the project, other crucial parts are to establish numerical models for mass transfer in COMSOL software. COMSOL served as significant roles of numerical approaches since it can provide with creative approaches to process intensification and use of innovative features in the design of microscale-based reactors and processes. The concentration profile of every species along both x-direction and y-direction can be obtained in the COMSOL model, which is significant and helpful to analyze the chemical process and transport phenomenon in the reactor. Based on the theoretical analysis, the inlet velocity of liquid reactant will affect the reaction rate and efficiency. In the COMSOL model, the concentration profile and the velocity profile along both x-direction and y-direction can be obtained. All COMSOL model results match mathematical model analysis and thus the parametric studies in COMSOL model can be used for future design to improve the reactor performance.

©Copyright by Pei Lun Zhang

Defense Date: November 21, 2018

All Rights Reserved

Dechlorination of Chlorinated Phenols in Microscale Based Reactor; Mathematical Model, and
Numerical Simulation

By

Pei Lun Zhang

A THESIS

Submitted to

Oregon State University

in partial fulfillment of
the requirements for the
degree of
Master of Science

Presented November 21, 2018

Commencement June 2019

Master of Science thesis of Pei Lun Zhang presented on November 21, 2018

APPROVED:

Major Professor, representing Chemical Engineering

Head of the School Chemical, Biological, and Environmental Engineering

Dean of the Graduate School

I understand that my thesis will become part of the permanent collection of Oregon State University libraries. My signature below authorizes release of my thesis to any reader upon request.

Pei Lun Zhang, Author

ACKNOWLEDGEMENTS

I really express my grateful appreciation to my major professor, Dr. Goran Jovanovic, to whom I owe very much in many respects. His outstanding and impressive teaching and instruction have motivated me to make a lot of progress and move forward to a successful career during my academic career. I won't forget what he taught to me on my project, which has affected me positively and profoundly in my future career.

I am also truly grateful for the unwavering support offered by my family. I must thank my father, Zhang Jian Wei since he supported my graduate studies financially and stand by my side during my challenging and struggling time. He was also of great support and gave me a lot of applicable advice when I was struck with problem in my life.

TABLE OF CONTENTS

	<u>Page</u>
1. INTRODUCTION	1
1.1 Chlorinated Compounds	1
1.2 Goals and Objectives	6
2. FUNDEMENTALS	7
2.1 Microscale-Based Technology	7
2.2 Flow Dynamic of P-chlorophenol in the Main Fluid	10
2.3 Characteristics Time Analysis of the Reactor	12
2.4 Stoichiometric Reaction for all Elemental Reactions	16
2.5 Chemical Kinetics for Elementary Reactions in the Gel Phase	24
3. MATHEMATICAL MODEL FOR MASS BALANCE	38
4. NUMERICAL SIMULATION OF THE MASS BALANCE	44
5. CONCLUSION	60
BIBLIOGRAPHY	61
APPENDICES	63

LIST OF FIGURES

<u>Figure</u>	<u>Page</u>
2.1 The simple illustration of the velocity of p-chlorophenol in the main fluid	10
2.2 The process of the first step of dechlorination	22
2.3 The process of the second step of dechlorination	22
2.4 The graphical representation for elementary reactions	28
3.1 The concentration of p-chlorophenol and phenol in the x-direction in the main fluid	45
3.2 The concentration of p-chlorophenol and phenol at the middle of the gel phase	46
3.3 The concentration of p-chlorophenol and phenol at the bottom of the gel phase	46
3.4 The concentration of p-chlorophenol in the y-direction at x=5mm	47
3.5 The concentration of phenol in the y-direction at x=5mm.....	47
3.6 The concentration of p-chlorophenol in the y-direction at x=10mm	48
3.7 The concentration of phenol in the y-direction at x=10mm.....	48
3.8 The concentration of p-chlorophenol in the y-direction at x=15mm	49
3.9 The concentration of phenol in the y-direction at x=15mm.....	49
3.10 The concentration of p-chlorophenol on the iron surface	50
3.11 The concentration of p-chlorophenol on the palladium surface	51
3.12 The concentration of hydrogen ions on the iron surface.....	52
3.13 The concentration of hydrogen radicals on the iron surface	53
3.14 The concentration of hydrogen molecules on the iron surface	54
3.15 The concentration of hydrogen molecules on the palladium surface	54
3.16 The concentration of hydrogen radicals on the palladium surface.....	55
3.17 The concentration of intermediate products on the palladium surface	56

LIST OF FIGURES (Continued)

<u>Figure</u>	<u>Page</u>
3.18 The concentration of phenol on the palladium surface	57
3.19 The concentration of iron surface.....	58
3.20 The concentration of palladium surface	58
3.21 The concentration of electrons on the catalyst surface	59

LIST OF TABLES

<u>Table</u>	<u>Page</u>
3.1 The final mass transfer equations for the species on the catalyst surface	43

LIST OF APPENDICES

<u>Appendix</u>	<u>Page</u>
A. Development of Navier-Stokes equation of p-chlorophenol in the main fluid.....	63
B. Development of mass balance equations of p-chlorophenol in the main fluid.....	65
C. Values of parameters in the COMSOL software	68
D. Development of mass balance equations of species on the catalyst surface.....	72
E. The screen images of the numerical model built up in the COMSOL software	76

NOMENCLATURE

$[H_2O]_{fluid}$	Water in the main fluid
$[H_2O]_{gel}$	Water in the liquid phase of the gel phase
$[H^+]_{fluid}$	Hydrogen ions in the main fluid
$[H^+]_{gel}$	Hydrogen ions in the liquid phase of gel phase
$[OH^-]_{fluid}$	Hydroxide ions in the main fluid
$[OH^-]_{gel}$	Hydroxide ions in the liquid phase of the gel phase
$[Fe^0]_{catalyst}$	The iron surface on the catalyst surface
$[Fe^{2+}]_{gel}$	Ferrous ions in the liquid phase of the gel phase
$[H_2]^o$	Hydrogen molecule associated with the iron surface
$[H_2]^*$	Hydrogen molecule associated with palladium surface
$[H_R]^*$	Hydrogen radical associated with palladium surface
$[R-Cl]_{fluid}$	P-chlorophenol in the main fluid
$[R-Cl]_{gel}$	P-chlorophenol in the liquid phase of gel phase
$[R-Cl]^o$	P-chlorophenol molecule associated with iron surface
$[R-Cl]^*$	P-chlorophenol molecule associated with palladium surface
$[R-HCl]^*$	Intermediate species associated with palladium surface
$[HCl]^*$	Hydrogen molecules associated with palladium surface
$[R]^*$	Phenol molecule associated with palladium surface
$[R]_{gel}$	Phenol molecule in the liquid phase of gel phase

L	The length of microscale-based scale reactor	$[m]$
d_1	The height of the main fluid in microscale-based scale reactor	$[m]$
d_2	The height of the gel phase in microscale-based scale reactor	$[m]$
S	The total area of Fe/Pd catalyst	$[m_c^2]$
S^o	Area of the iron surface substrate on the catalyst surface	$[m_{s^o}^2]$
S^*	Area of palladium surface on the catalyst surface	$[m_{s^*}^2]$
$\frac{S^o}{S}$	The fraction of the catalyst surface containing surface of the iron surface substrate	$\left[\frac{m_{s^o}^2}{m_c^2}\right]$
$\frac{S^*}{S}$	The fraction of the catalyst surface containing palladium surface	$\left[\frac{m_{s^*}^2}{m_c^2}\right]$
V_g	The volume of the gel phase	$[m_g^3]$
$\frac{S}{V_g}$	The total surface area of catalyst per volume of the gel phase	$\left[\frac{m_c^2}{m_g^3}\right]$
$(u_x)_{[R-Cl]_{fluid}}$	The flow rate of p-chlorophenol in the main fluid	$[m/s]$
$(u_x)_{[R]_{fluid}}$	The flow rate of phenol in the main fluid	$[m/s]$
D_1	The diffusion coefficient in the main fluid	$\left[\frac{m^2}{s}\right]$

D_2	The diffusion coefficient in the gel phase	$\left[\frac{m^2}{s} \right]$
τ_L	Mean residence time of p-chlorophenol in the microscale-based reactor	$[s]$
τ_{D_1}	Diffusion time of p-chlorophenol in the main fluid in microscale-based scale reactor	$[s]$
τ_{D_2}	Diffusion time of p-chlorophenol in gel part in microscale-based scale reactor	$[s]$
$\tau_{[R-Cl]_{gel} \rightarrow [R-Cl]^o}$	The reaction time of adsorption of p-chlorophenol molecules to iron surface substrate	$[s]$
$\tau_{[R-Cl]_{gel} \rightarrow [R-Cl]^*}$	The reaction time of adsorption of p-chlorophenol molecules to palladium surface	$[s]$
$\tau_{[R-Cl]^o \rightarrow [R-Cl]^*}$	Reaction time for migration of p-chlorophenol from the iron surface substrate to palladium surface	$[s]$
$\tau_{[R-Cl]^* \rightarrow [R-HCl]^*}$	Reaction time for the first step of dechlorination of p-chlorophenol at palladium surface	$[s]$
$\tau_{[R-HCl]^* \rightarrow [R]^*}$	Reaction time for the second step of dechlorination of p-chlorophenol	$[s]$
τ_r	Reaction time for the whole dechlorination process	$[s]$
k_1	The inlet rate Constant of dissociation of water in the gel phase	$\left[\frac{mol}{m^3 \cdot s} \right]$

k_2	The rate constant of irreversible dissociation of water in the gel phase	$\left[\frac{\text{mol} [OH^-]_{gel}}{m_g^3 \cdot s} \right]$
k_8	The rate constant of production of hydrogen ions on the zero-valent substrate	$\left[\frac{m_c^2}{m_{s^o}^2 \cdot s} \right]$
k_9	The rate constant of migration of hydrogen ions from the zero-valent substrate to palladium surface	$\left[\frac{m_c^2}{m_{s^*}^2 \cdot s} \right]$
k_{10}	The rate constant of production of hydrogen ions on a palladium surface	$\left[\frac{m_c^2}{m_{s^*}^2 \cdot s} \right]$
k_{11}	The rate constant of production of hydrogen radicals on a palladium surface	$\left[\frac{1}{s} \right]$
k_{12}	The rate constant of production of hydrogen radicals on the zero-valent substrate	$\left[\frac{1}{s} \right]$
k_{13}	The rate constant of production of hydrogen molecules on the zero-valent substrate	$\left[\frac{m_c^2}{m_{s^o}^2 \cdot s} \right]$
k_{14}	The rate constant of migration of hydrogen molecules from the zero-valent substrate to palladium surface	$\left[\frac{m_c^2}{m_{s^*}^2 \cdot s} \right]$
k_{15}	The rate constant of desorption of hydrogen molecules to the zero-valent substrate.	$\left[\frac{1}{s} \right]$
k_{16}	The rate constant of adsorption of hydrogen molecules to the zero-valent substrate	$\left[\frac{m_c^2}{m_{s^o}^2 \cdot s} \right]$
k_{17}	Rate Constant of direct absorption of hydrogen molecules to palladium surface	$\left[\frac{m_c^2}{m_{s^*}^2 \cdot s} \right]$

k_{18}	The rate constant of disassociation of hydrogen molecules associated with palladium surface	$\left[\frac{1}{s} \right]$
k_{19}	The rate constant of adsorption of p-chlorophenol molecules to the zero-valent substrate	$\left[\frac{m_c^2}{m_{s^0}^2 \cdot s} \right]$
k_{20}	The rate constant of desorption of p-chlorophenol to palladium surface	$\left[\frac{1}{s} \right]$
k_{22}	The rate constant of direct absorption of p-chlorophenol to palladium surface	$\left[\frac{m_c^2}{m_{s^*}^2 \cdot s} \right]$
k_{21}	The rate constant of migration of p-chlorophenol molecules from the zero-valent substrate to palladium surface	$\left[\frac{m_s^2}{m_{s^*}^2 \cdot s} \right]$
k_{23}	The rate constant of first-step disassociation of p-chlorophenol on the palladium surface	$\left[\frac{m_c^2}{mol[H_R]^* \cdot s} \right]$
k_{24}	The rate constant of second-step disassociation of p-chlorophenol on the palladium surface	$\left[\frac{m_c^2}{mol[H_R]^* \cdot s} \right]$
k_{25}	The rate constant of direct desorption of phenol from palladium surface to gel phase	$\left[\frac{1}{s} \right]$
k_{26}	The rate constant of direct desorption of hydrogen chloride from the palladium surface to gel phase	$\left[\frac{1}{s} \right]$

Dechlorination of Chlorinated Phenols in Microscale Based Reactor; Mathematical Model, and Numerical Simulation

Chapter 1 Introduction

1.1 Chlorinated Compounds

Industries should be responsible for contributing to worldwide pollution because they are driven by profit maximization and market domination instead of focusing on the environment. Economic growth and a cleaner environment seem mutually exclusive. Achieving a balance is possible if human beings carefully consider how to use advanced technology to spur economic growth and solve ecological challenges at the same time. In particular, industries develop chlorophenol compounds and derivatives, which are used as intermediates in many industrial processes, such as in the manufacturing of paper products, plastics, and dyes. Such development is not without consequences though, for it negatively affects the environment by generating many pollutants.

Chlorophenol is widely used in many industries. For example, chlorinated compounds play a significant role in wood preservation. Chlorophenol acts to protect wood from attacking by discoloring fungi, and against fungal decay. Consequently, a large amount of waste containing chlorinated compounds is generated during the pre-processing of wood. Additionally, the chlorophenol is crucial in water disinfection. Chlorophenol serves as disinfection of drinking water by chlorinating. It also serves to guarantee the safety of public swimming pools, because it can prevent waterborne pathogens from growing, which protects swimmers' ears and skin from

infection. Moreover, chlorinated organics are used in the paper industry. Many chlorine and chlorinated compounds are treated as a bleaching agent. Compared to other industrial usages, most of the chlorine consumed by the public is due to the bleaching of paper pulps. The usage of chlorinated compounds in paper industry accounts for approximately sixty-five percent of the total amount.

As discussed in the examples of above, there are widespread industrial usages of chlorinated compounds. The ubiquity of chlorophenol and their derivatives in everyday life presents many issues due to their toxicity and suspected carcinogenicity (M. Ahmaruzzaman 2004). For instance, once released into the environment, chlorinated organics will accumulate in the surroundings and endanger human as well as the ecological environment over time (R.P. Schwarzenbach 1976). Chlorinated phenols are toxic since they can penetrate human skin and epithelium, causing damage and necrosis. Chlorinated aromatics like benzenes are difficult to biodegrade and tend to accumulate in animal tissue (Yang, Lei 2011). Exposure to chlorophenol through dermal contact, inhalation, and ingestion is harmful to both humans and animals. Long-term exposure to the chlorinated phenols can lead to some symptoms, such as convulsions and oxidative phosphorylation. Workers continually exposed to chlorophenol are more likely to get asthma, heart disease, chromosomal aberrations, malignant mesothelioma, and lung cancer. People who drink water contaminated with chlorophenol could increase the risk of digestive tract infections, asthma, depression, and morbidity. Moreover, ingestion of chlorinated phenol can cause health conditions such as myocardial ischemia and lymphoma. Additionally, high-level concentrations of

PCP commonly used in pesticides and solvents have the potential to cause T-lymphocyte dysfunction.

Chlorophenol pollution not only harms humans but also threatens the water system and air quality. As mentioned before, the chlorinated compounds released from different industrial processes such as pulp bleaching, water disinfection or even waste incineration, are harmful. Once chlorinated phenol enters the water system, including the surface and ground waters in nature, it will stay in the water table for a long period, since chlorinated compounds are highly resistant to biodegradation. Moreover, the pollution of chlorinated compounds in the air is concerning, since chlorophenol is emitted in the atmosphere in vapor form during chlorophenol production, which can cause acid rain.

Fortunately, scientists have recognized the severity of the negative influence caused by chlorinated compounds. Numerous environmental organizations have been established in many countries to inform and educate the public regarding the harmful effects of excessive chlorine usage. These organizations have worked to inform governments of this problem, which has resulted in efforts to enact legislation to regulate industrial emissions. Increasingly, citizens realize the importance of reducing pollution. Therefore, the growth of attention to environmental pollution caused by the usage of chlorophenol has led to developments in technology that help deal with the problems caused by chlorinated compounds. For example, vitrification can eliminate chlorinated compounds in soil. The advantage of vitrification is that it addresses mixed waste sites and reduces chlorinated

compounds in soil volume. The disadvantage is that it must address the final disposal issue and once disposed, the land may not be usable. Thermal desorption is another way to treat chlorophenol compounds in soil. The benefit of this approach is that it is applicable to a variety of soils including low permeability clays of a heterogeneous nature. The drawback is that it has slow desorption from recalcitrant fractions, which presents disposal issues. The final approach is soil washing, which can eliminate chlorophenol compounds in soil. The advantage of washing is that hydrophilic organics can be easily removed, and it can remove a wide range of compounds, but the highly hydrophobic compounds may require a surfactant and it must address the final disposal issue of the secondary waste stream. Moreover, how to dechlorinate in water is another concern. Activated carbon sorption is one of the common ways to deal with chlorophenol compounds in water. The advantage is a high adsorption capacity for chlorinated and non-chlorinated organics and excellent trace concentration removal, but the regeneration by incineration is a potential hazard for dioxin formation. The other way is catalytic dechlorination. It can completely dechlorinate a variety of aromatic and straight chain compounds. Fast dechlorination rates for both high and low inlet contamination concentration is advantageous. Yet, the lifetime and deactivation of the catalyst may affect the process and the approach is not cost-effective.

Apart from these common traditional ways, metal-enhanced dechlorination is a creative technology attracting attention since it is superior to most of the conventional ways. Among single-metal dechlorination, iron surface iron has been explored as a remedial and creative agent for chlorinated organic compounds in groundwater (W.S. Orth 1996). However, single iron surface iron results in many challenges: the dechlorination rate will decrease because of the production of

byproducts on the surface. In order to improve the performance of single metal dechlorination, various bimetallic particles such as Pd/Fe, Ni/Fe, and Cu/Fe have been synthesized and used to improve the reactivity and functionality of the ZVI (Huang, Q 2013), increasing the efficiency of dechlorination. For example, the Pd metal can serve as a catalyst to adsorb H_2 generated from the iron corrosion and further decompose H_2 into atomic H for highly efficient dechlorination. (Yang, L 2011)

Additionally, the iron surface or bimetallic particles are very easy to agglomerate (Huang, Q 2013), and thus the activity of Pd/Fe catalyst will decrease. Further, agglomeration causes challenges in recovering nanoparticles from gel solution after the Pd/Fe catalyst treats the wastewater (H. Kim 2008). In the thesis, several innovative technologies are used to solve this shortcoming and improve the performance of Pd/Fe catalyst. Firstly, the nanoparticles of Pd and Fe are mixed with water, which not only reduces the potential agglomeration of nanoparticles but also can highly reduce the diffusion resistance of p-chlorophenol in the gel part. Another advantage is that the gel form of the catalyst is fixed on the reaction plates in the reactor, making it easier to recycle, since if the catalyst is in gel form, it will mix with p-chlorophenol and leaves the reactor. Immobilizing and stabilizing Pd/Fe catalyst can eventually contribute to the activity of dechlorination.

1.2 Goals and Objective

Goals:

- Explore the fluid dynamic of the p-chlorophenol in the reactor, including diffusion and convection.
- Study the elementary reactions for the dechlorination of p-chlorophenol with Pd/Fe catalyst.
- Create a mathematical model, which can successfully describe the dechlorination reaction process, including chemical kinetics, flow dynamics, characteristic time analysis, and mass balance.

Objectives

- Develop a mathematical model for the chemical kinetics, characteristic time analysis and mass balance equations in the micro-scale based reactor with an immobilized Pd-Fe catalyst.
- Study the acceptable and reasonable constants involved in the elementary reactions
- Simulate chemical kinetics for every species with COMSOL software

Chapter 2 Fundamentals

2.1 Microscale-Based Technology

Microtechnology is a technology on a small or microscopic scale (1 micrometer, or 10^{-6} meter). It is also a study, which looks at the development and application of devices whose operations are based on the scale of 1-100 microns. A microscale-based reactor is generally defined as a miniaturized reactor with characteristic dimensions in micrometers and reaction volumes in the nanoliter-to-microliter range (Zhang, X 2001). In particular, the microscale-based reactor is a recent development and is considered a creative reactor type. This reactor type requires more sophisticated and advanced technology to design it. Building these reactors is worth doing though because it has seemingly unlimited potential in industrial applications. More generally, it signals a promising future for chemical engineering research. For example, increasing research efforts and growing industrial interest in microscale technology for continuous-flow manufacturing (Newman, S.G 2013) sheds new light on basic process development. Moreover, the micro-scale based reactor offers a new paradigm for chemical production (Hessel, V. et al 2013) because it is likely to trigger a revolution in chemical engineering manufacturing and shorten the gap between the laboratory and large-scale processing.

Microscale reactors have many general advantages. Firstly, they are safe and environmental-friendly. For example, traditional chemical manufacturing, such as a chemical bath reactor, commonly produces toxic or hazardous materials. However, integrated microfluidic systems improve safety, health and the environment (Wohlgemuth, R 2015). Due to good selectivity and

high efficiency, the by-products that microscale-based reactors produce declines, which can contribute to a cleaner environment.

Secondly, microtechnology has a larger surface to volume ratio compared with large-scale chemical engineering reactors in industry. This benefit can obviously increase heat and mass transfer and decrease diffusion paths. Many micro-based scale channels increase the surface of transferring energy, and thus the heat energy in the reactor can transfer more evenly. Therefore, improving the efficiency of heating transfer contributes to a more accurate understanding of the influence of temperature. The larger surface to volume ratio also enables improved catalytic efficiency, to overcome the thermodynamic limitation, and to enhance product purity (Wohlgemuth, R 2015), reducing the operating cost and production cost.

Finally, the model of the microscale-based reactor is flexible. Different from the conventional reactors like a batch reactor, a microscale-based reactor can be easily assembled and disassembled, which allows us to design more configurations or shapes of reactors. These models for micro-scale based reactors can be manufactured more easily, which save a great deal of time. Additionally, the flexibility of microscale-based reactors increases the variety of integration with other systems. The smaller scale reactors can lead to decreased costs of fabrication compared with the traditional reactor. In my project, higher conversion, selectivity, and efficiency of small channels in the micro-scale based reactor encourage engineers to use it instead of a conventional batch experiment. The micro-scale reactor is advantageous for catalytic reactions occurring on the inner surfaces of

the microchannel and monolithic reactors with the immobilized catalyst (Wohlgemuth, R 2015). Moreover, since chemicals in the main fluid include reactant p-chlorophenol and phenol, some derivate of chlorophenol, as by-products, are likely to be produced. The small volume of the micro-scale based reactor is helpful to control the number of toxic waste yields. In addition, the micro-scale volume can reduce the viscosity of the reactant flows. The influence of flow dynamics is crucial because the reactants p-chlorophenol needs to diffuse from the gel phase to gel part and then react with hydrogen radicals, but a shorter diffusion path in a micro-scale based reactor is helpful to reduce it.

2.2 Flow Dynamic of P-chlorophenol in the Main Fluid

The p-chlorophenol flows into the microscale-based reactor in the x-direction, and thus the velocity of the p-chlorophenol is along the x-direction. Based on the previous assumption the p-chlorophenol can be treated as a laminar flow in the gel phase. From figure 2.1, the microscale-based reactor can be simply considered as two parallel plates. Therefore, the Navier Stokes equation can be applied. The final simplified equation of velocity of p-chlorophenol is

$$\frac{\partial P}{\partial x} = \mu \left(\frac{\partial^2 u_x}{\partial y^2} \right) \text{ (the process of simplifying Navier-Stokes equations is developed in Appendix A)}$$

and the solution to the equation can be easily got. The constants a and b can be solved by two boundary conditions.

$$u_x = \frac{P_{x=L} - P_{x=0}}{2\mu} y^2 + ay + b \quad (\text{Eq.2.1})$$

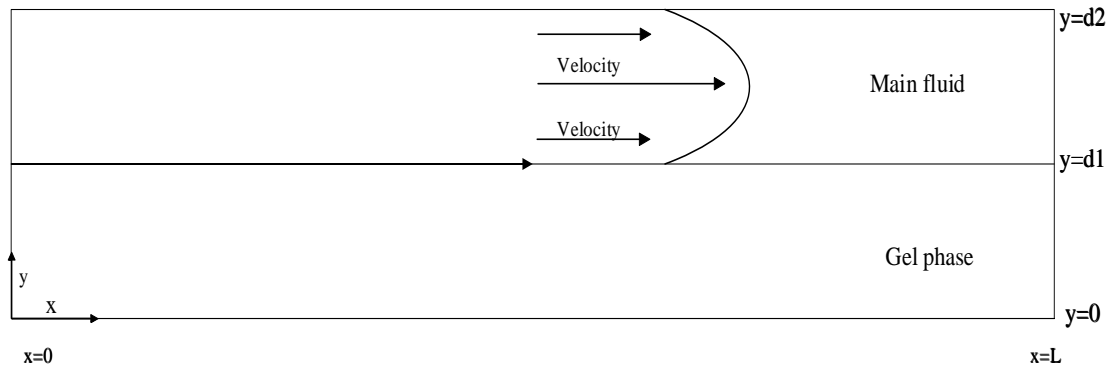


Figure 2.1 The simple illustration of the velocity in the main fluid

The first boundary condition can be obtained, when the p-chlorophenol is at the entrance of the microscale-based reactor. Since there is the closed wall at $y = 0$, the velocity of p-chlorophenol is equal to zero. The boundary condition can be expressed by:

$$BC1): y = d_2, u_x = 0 \quad (\text{Eq.2.2})$$

The second boundary condition can be obtained through the velocity profile of laminar flow in two plates. The velocity of p-chlorophenol at the center of the two plates is supposed to be half of the maximum velocity. Besides, the flux of p-chlorophenol $y = d_1$ should be equal to zero.

Therefore, the boundary condition can be expressed by:

$$BC2): y = \frac{d_2 - d_1}{2}, \frac{\partial u_x}{\partial y} = 0 \quad (\text{Eq.2.3})$$

When the first boundary condition is applied, and the second boundary condition is applied, the final solution of the velocity of p-chlorophenol can be expressed:

$$u_x = \frac{P_{x=L} - P_{x=0}}{2\mu L} y^2 + \frac{(d_1 - d_2)(P_{x=L} - P_{x=0})}{2\mu L} y - \frac{P_{x=L} - P_{x=0}}{2\mu L} d_2^2 - \frac{(d_1 - d_2)(P_{x=L} - P_{x=0})}{2\mu L} d_2 \quad (\text{Eq.2.4})$$

2.3 Characteristics Time Analysis of the Reactor

Investigating the characteristics time of microscale-based reactor with can estimate the performance of a microscale-based reactor and argue advantages of it. Therefore, the time scale analysis is always treated as an efficient tool to assess the design of a microscale-based reactor. A series of parameters affect the characterization of the performance of the reactor. These things include: flow dynamic of laminar flow, mass transfer diffusion and reaction rate. The characteristics times include reaction time, residence time, and diffusion time. In my thesis, the microscale-based has the length L , the height of the main fluid d_1 and the height of the gel part d_2 . The diffusion coefficient of the reactants $[R-Cl]_{fluid}$ in the main fluid is D_1 . The average velocity of $[R-Cl]_{fluid}$ in the main fluid is u_{ave} . The reactants $[R-Cl]_{fluid}$ diffuse into the gel part. The diffusion coefficient of the reactants $[R-Cl]_{fluid}$ in the gel part is D_2 . The reactants will react with catalyst when they diffuse in the gel part. The reactions include the adsorption of $[R-Cl]_{gel}$. Analyzing the chemical reaction process often related to a series of reaction, and thus it is crucial to determine the critical step as a controlling step in the complete chemical reaction process rate.

These characteristic times can help us to estimate if microscale-based reactor approach to chemical reaction is feasible. If these characteristic times are not feasible, we need to figure out how to change the parameters of the microscale-based reactor to make them sense. For example, we can control the mean residence time by changing the length of the microchannel or the average velocity of the fluid. Besides, the diffusion time also can be increased when we increase the radius of the

microscale-based reactor. Since the diffusion coefficient depends on the environment where the reactants A exist, changing the diffusion coefficient will not work well. Moreover, the reaction time also can be affected by changing the volume or the surface area of the microchannel. The temperature influences the reaction rate constant, and thus growth or decline of temperature can affect the reaction time. The rough estimation can contribute to the designing of the microscale-based reactor and build up the mathematical model in this thesis.

The mean residence time represents the time that reactants A need to flow with the average velocity u in the x-direction from the entrance to the end of the microchannel. The residence time is equal to the ratio of the length of the microchannel to the average velocity of the fluid. The residence time can be expressed by:

$$\tau_L = \frac{L}{u_{ave}} [s] \quad (\text{Eq.2.5})$$

The diffusion time represents the time that the reactants A take to diffuse from the center of the microchannel to the wall. The diffusion time is considered as important parameters since it determines when the surface reaction will happen. The diffusion time is equal to the ration of radium square to the diffusion coefficient. Express the diffusion time in the main fluid:

$$\tau_{D_1} = \frac{d_1^2}{D_1} [s] \quad (\text{Eq.2.6})$$

Similarly, the diffusion of reactants also occurs in the gel part, but the diffusion coefficient is slightly different because there is catalyst existing apart from the water. The diffusion time in the gel part can be represented by:

$$\tau_{D_2} = \frac{d_2^2}{D_2} [s] \quad (\text{Eq.2.7})$$

Chemical reactions are not infinitely fast since there will be a reaction time needed for the p-chlorophenol in the main fluid transforming to the product phenol in the gel phase. Since there are several reactions occurring on the catalyst, some of which are parallel reactions and others are consecutive reactions. The reaction time is determined by the critical reaction process. Figure 2.3 clearly shows the relationship of every reaction. The adsorption of p-chlorophenol and of hydrogen are parallel reactions. However, the first step of dechlorination and the second step of dechlorination are consecutive reactions. According to the units, the reaction time can be obtained through the ordinary reaction rate constant. The reaction time for adsorption of reactants can be expressed by:

$$\tau_{[R-Cl]_{gel} \rightarrow [R-Cl]^o} = \frac{S}{S^o} \cdot \frac{1}{k_{[R-Cl]_{gel} \rightarrow [R-Cl]^o}} [s] \quad (\text{Eq.2.8})$$

The reaction time for direct adsorption of reactants can be expressed by:

$$\tau_{[R-Cl]_{gel} \rightarrow [R-Cl]^*} = \frac{S}{S^*} \cdot \frac{1}{k_{[R-Cl]_{gel} \rightarrow [R-Cl]^*}} [s] \quad (\text{Eq.2.9})$$

The reaction time for the first step of dechlorination of reactants can be expressed by:

$$\tau_{[R-Cl]^* \rightarrow [R-HCl]^*} = \frac{1}{k_{[R-Cl]^* \rightarrow [R-HCl]^*}} [s] \quad (\text{Eq.2.10})$$

The reaction time for the second step of dechlorination of reactants can be expressed by:

$$\tau_{[R-HCl]^* \rightarrow [R]^*} = \frac{1}{k_{[R-HCl]^* \rightarrow [R]^*}} [s] \quad (\text{Eq.2.11})$$

The reaction time for phenol leaving from the palladium surface can be expressed by:

$$\tau_{[R]^* \rightarrow [R]_{gel}} = \frac{1}{k_{[R]^* \rightarrow [R]_{gel}}} [s] \quad (\text{Eq.2.12})$$

Compared to the time of adsorption and migration of p-chlorophenol and hydrogen, the process of dechlorination takes much more time. Further, the state of $[R-Cl]^*$ is more steady than intermediate species $[R-HCl]^*$. Therefore, the time for the first step of dechlorination is much longer than the second step of dechlorination and thus the first step of dechlorination should be the critical reaction. The whole reaction time can be obtained:

$$\tau_r = \tau_{[R-Cl]^* \rightarrow [R-HCl]^*} = \frac{1}{k_{[R-Cl]^* \rightarrow [R-HCl]^*}} [s] \quad (\text{Eq.2.13})$$

Based on the equations for four-time constants, the mean residence time of main fluid is supposed to be the largest characteristic time and thus the reactant p-chlorophenol should have enough time to diffuse to gel part and react with the catalyst. Further, the time that reactants p-chlorophenol takes to diffuse from the gel phase to the catalyst surface, τ_{D_2} should be approximately equal to the reaction time τ_r . The result of the relationship among these characteristic times suggest:

$$\tau_L > \tau_{D_1} > \tau_{D_2} \approx \tau_r [s] \quad (\text{Eq.2.14})$$

2.4 Stoichiometric Reaction for all Elemental Reactions

The types of solid catalyzed reaction processes are various due to the different catalysts and reactants. Therefore, the representations of the catalyzed process are wide-ranging. In order to understand and simulate the catalyzed process, an accurate mathematical model for chemical kinetics should be established. The mathematical model should include the elementary reaction occurring on the catalyst surface and the differential equations that can represent the reaction rate of different reactions or the transfer of each species on the catalyst surface. The accuracy of the mathematical model is dependent on the complexity of the catalyzed process. Then, the way to justify the model is to compare how well it aligns with the sufficient and resolute experimental data. The degree to which the mathematical model fits the practical experimental data determines the direction in revising the model representations.

In addition to assuring the accuracy of the mathematical model, we also need to allow the model to be calculable. Consequently, sufficient and reasonable assumptions should be set up to simplify the model. A simplified model can efficiently investigate the design of reactors, the whole process of reactions and the chemical reaction rates for every species. In addition, a satisfactory model can more precisely predict the reaction process at each step or the change of chemical reaction rates under different reaction conditions. As a result, a successful model also can contribute to improving the performance of microscale-based reactors and increase the reaction rate or final conversion.

To explain the principle of the chemical kinetics for p-chlorophenol in the micro-scale based reactor more thoroughly, it is crucial to create a graphical representation of the solid catalyzed reaction, investigate elementary reactions and develop first-order chemical kinetics for every species. Figure 2.1 shows the solid catalyzed reaction process of p-chlorophenol. The p-chlorophenol molecules diffuse from the main fluid to the gel phase. Then p-chlorophenol molecules are adsorbed on the surface of the iron surface substrate to form reactant molecules associated with the iron surface substrate $[R-Cl]^o$. These $[R-Cl]^o$ migrate to palladium surface, becoming species associated with palladium surface $[R-Cl]^*$. Additionally, the reactant molecules in the gel phase can be directly adsorbed on the palladium surface on the catalyst surface to form $[R-Cl]^*$.

When the hydrogen radical $[H_R]^*$ produced at the palladium surface that is around the Palladium, the first step of dechlorination starts. The $[R-Cl]^*$ will dechlorinate to the intermediate products $[R-HCl]^*$. These intermediate products cause the second step of dechlorination, and thus the final production of phenol associated with palladium surface $[R]^*$, and hydrogen chloride associated with palladium surface $[HCl]^*$, are produced. The force between the products and palladium surface are too weak to fix the phenol molecules, so $[R]^*$ and $[HCl]^*$ are desorbed from the catalyst surface to the gel phase.

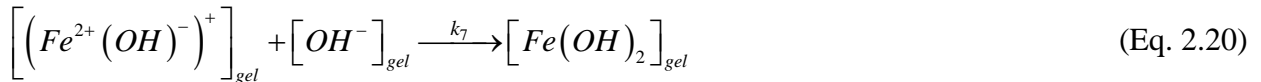
In order to study the whole process of the dechlorination, figuring out the elementary reactions in the reactor is an effective method. The reactants p-chlorophenol diffuse from the main fluid to the catalyst phase due to the difference of concentration, however, there is no dechlorination before the p-chlorophenol flows into the gel phase. Therefore, the only reaction in the main fluid is the dissociation of water. The dissociation of water also happens in the gel phase, since the most part of the gel phase is water. The water molecule dissociates to hydrogen ions and hydroxyl ions and the process can be expressed by the equation:



When $[(Fe)^{2+}]^o$ diffuses into the liquid phase of the gel phase, it reacts with hydroxide to the

product $[(Fe^{2+}(OH)^-)^+]_{gel}$ that can continue to react with hydroxide to produce ferrous

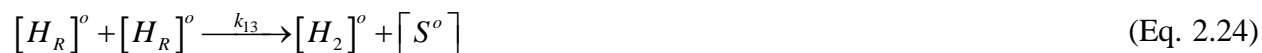
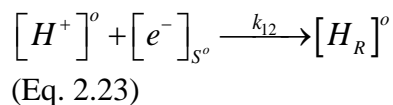
hydroxide:



The hydrogen ions in the liquid phase of the gel phase can be adsorbed onto the iron surface and then these hydrogen ions can migrate from the iron surface to the palladium surface. The two processes can be expressed by the two equations:



The hydrogen ions on the iron surface can get electrons from the process of transferring iron to the ferrous ions, forming hydrogen radicals on the iron surface. Since hydrogen radicals are very active, the two hydrogen radicals are easily combined to form hydrogen molecules on the iron surface. The process can be expressed by the two equations:



However, the desorption of hydrogen molecules associated with the iron surface substrate also occurs, since the force between the hydrogen and iron is not very strong. The Fe^0 on the catalyst serves as the reducing agent forming an effective redox couple with water yielding ferrous iron and hydrogen gas (W.A. Arnold 2000). Once the hydrogen gas is adsorbed on the iron surface substrate, it migrates from iron surface substrate to palladium surface and affixed with palladium surface to form surface hydrogen molecules $[H_2]^*$. The process is the migration of hydrogen molecules:



Due to the characteristics of Pd, the dissociation of H₂ on the Pd leads to the formation of hydrogen radicals for the dechlorination reaction (X.Y. Wang 2008). One hydrogen molecule can be stretched to two hydrogen radicals in Pd metal, because of the molecular force between the Pd molecules and hydrogen molecule, the hydrogen radical affixed with active surface sites can be defined as surface hydrogen radicals $[H_R]^*$. The process is represented by:



Apart from the adsorption of hydrogen ions onto the iron surface, they also can be adsorbed on the palladium surface. Similarly, the hydrogen ions also can get the electrons to form hydrogen radicals on the palladium surface:



The p-chlorophenol in gel phase associated with the iron surface substrate on the catalyst surface, forming $[R-Cl]^o$, which is defined as adsorption of p-chlorophenol molecules:



Once the p-chlorophenol molecules are adsorbed on the iron surface substrate $[R-Cl]^o$ can migrate on the catalyst surface and affixed with palladium surface. The p-chlorophenol molecules

can migrate from the surface of the iron surface substrate to the palladium surface on the catalyst surface, forming the $[R-Cl]^*$, which is defined as activation of the p-chlorophenol molecule



Some of the p-chlorophenol molecules directly occupy the palladium surface on the catalyst surface, forming $[R-Cl]^*$, which is defined as the direct adsorption of p-chlorophenol molecules:



After formation of $[R-Cl]^*$ the hydrogen associated with palladium surface reacts with them.

Since the structure of the p-chlorophenol, the double carbon bonds bounded with chloride is active. Consequently, the hydrogen radicals react with the double bonds, the species $[R-HCl]^*$ is formed:



The hydrogen radicals can continue to react with the product $[R-HCl]^*$. The final products phenol associated with palladium surface $[R]^*$ and hydrogen chloride associated with palladium surface $[HCl]^*$ are created. The phenol can leave the palladium surface to the gel phase and diffuse to the main fluid:



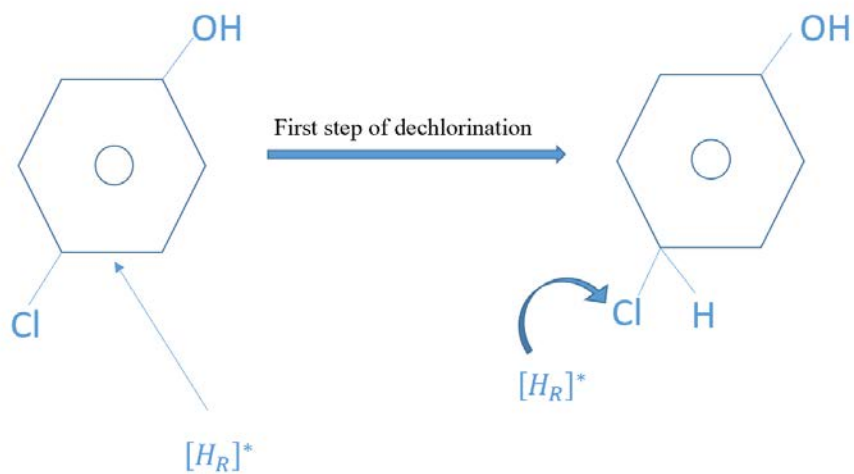


Figure 2.2 The process of the first step of dechlorination

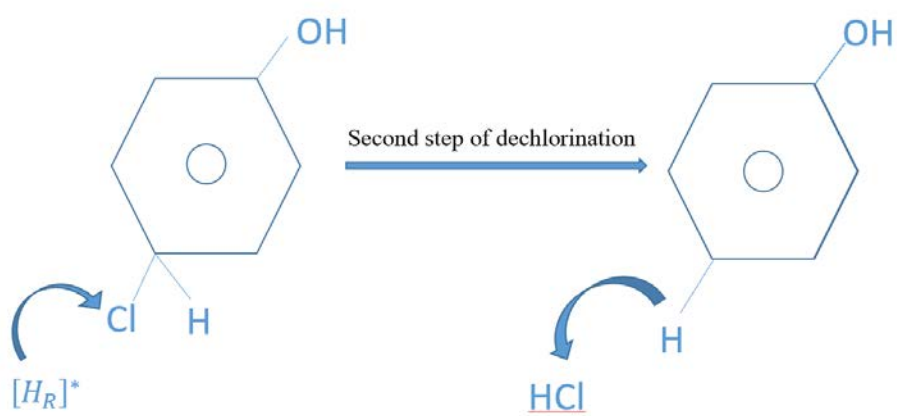


Figure 2.3 The process of the second step of dechlorination

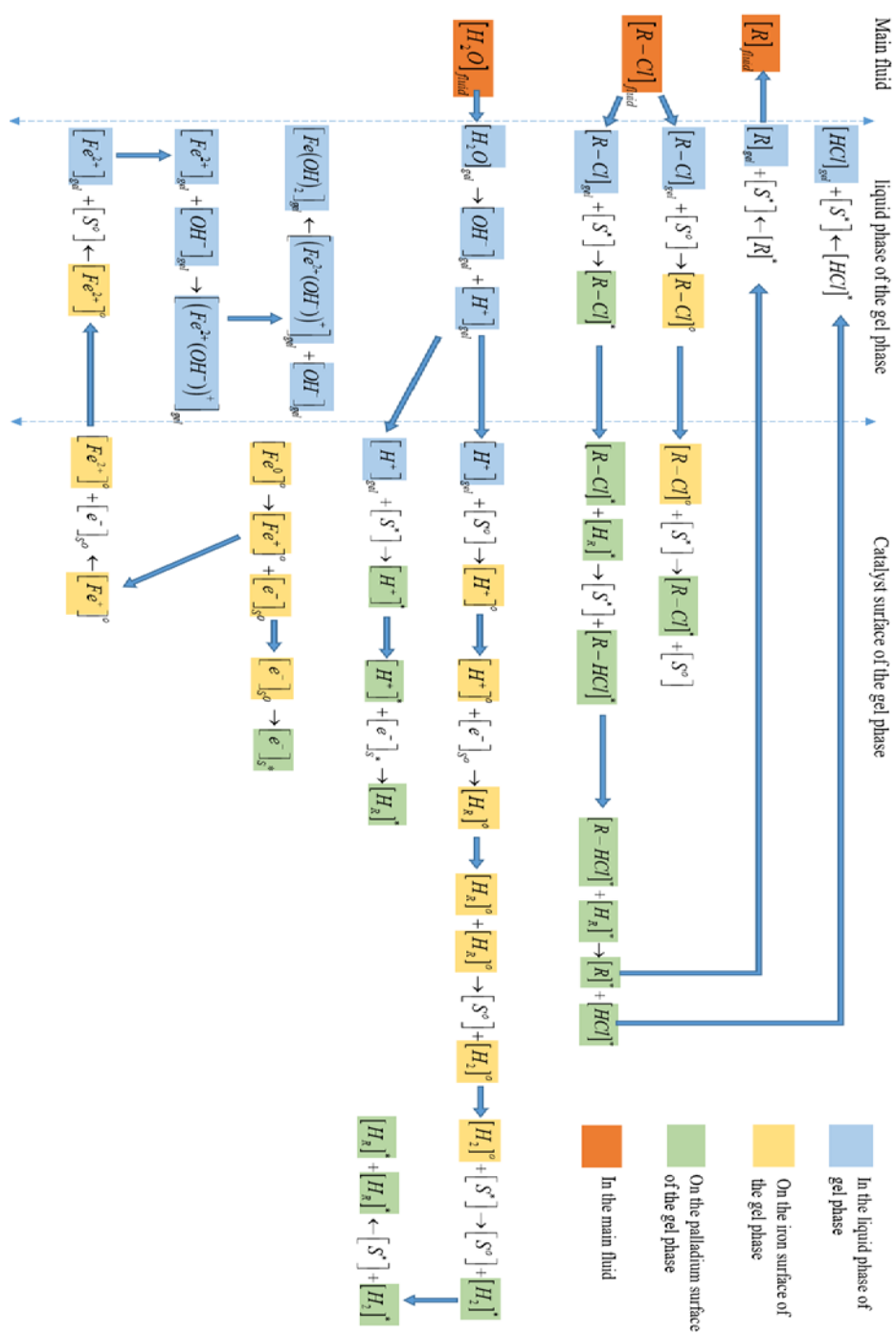


Figure 2.4: The graphical representation for elementary reactions

2.4 Chemical Kinetics for Elementary Reactions in the Gel Phase

Chemical kinetics of hydrogen molecules on the iron surface substrate $[H^+]^o$:

The hydrogen ions H^+ in the liquid phase of the gel phase can occupy the iron surface and produce the hydrogen ions on the iron surface $[H^+]^o$. The production of $[H^+]^o$ is expressed by:

$$r_{[H^+]_{gel} \rightarrow [H^+]^o} = \frac{dC_{[H^+]^o}}{dt} = k_8 \cdot C_{[H^+]_{gel}} \cdot \frac{S^o}{S} \cdot \zeta_{[H^+]_{gel} \rightarrow [H^+]^o} \cdot \frac{V_r}{S} \left[\frac{mol [H^+]^o}{m_{S^o}^2 \cdot s} \right] \quad (\text{Eq. 2.36})$$

The concentration of hydrogen ions on the iron surface $[H^+]^o$ decrease because they can combine with the electrons on the iron surface to generate the hydrogen radicals. The consumption of $[H^+]^o$ is expressed by:

$$-r_{[H^+]^o \rightarrow [H_R]^o} = -\frac{dC_{[H^+]^o}}{dt} = k_{12} \cdot C_{[H^+]^o} \left[\frac{mol [H^+]^o}{m_{S^o}^2 \cdot s} \right] \quad (\text{Eq. 2.37})$$

The net chemical kinetics of the $[H^+]^o$ can be represented:

$$\begin{aligned} \Delta r_{[H_2]^o} &= r_{[H^+]_{gel} \rightarrow [H^+]^o} - r_{[H^+]^o \rightarrow [H_R]^o} \\ &= k_8 \cdot C_{[H^+]_{gel}} \cdot \frac{S^o}{S} \cdot \zeta_{[H^+]_{gel} \rightarrow [H^+]^o} \cdot \frac{V_r}{S} - k_{12} \cdot C_{[H^+]^o} \left[\frac{mol [H^+]^o}{m_{S^o}^2 \cdot s} \right] \end{aligned} \quad (\text{Eq. 2.38})$$

Chemical kinetics of the hydrogen ions on the palladium surface $[H^+]^*$:

The concentration of hydrogen ions on the palladium surface $[H^+]^*$ increase because hydrogen ions in the liquid phase of the gel phase can diffuse to the palladium surface. The production of $[H^+]^*$ is expressed by:

$$r_{[H^+]_{gel} \rightarrow [H^+]^*} = \frac{dC_{[H^+]^*}}{dt} = k_{10} \cdot C_{[H^+]_{gel}} \cdot \frac{S^*}{S} \cdot \zeta_{[H^+]_{gel} \rightarrow [H^+]^*} \cdot \frac{V_r}{S} \left[\frac{mol[H^+]^*}{m_{S^o}^2 \cdot s} \right] \quad (\text{Eq. 2.39})$$

The concentration of hydrogen ions on the palladium surface $[H^+]^*$ decrease because they can combine with the electrons to generate the hydrogen radicals on the palladium surface. The consumption of $[H^+]^*$ is expressed by:

$$-r_{[H^+]^* \rightarrow [H_R]^*} = -\frac{dC_{[H^+]^*}}{dt} = k_{11} \cdot C_{[H^+]^*} \left[\frac{mol[H^+]^*}{m_c^2 \cdot s} \right] \quad (\text{Eq. 2.40})$$

The net chemical kinetics of the $[H^+]^*$ can be represented:

$$\begin{aligned} \Delta r_{[H^+]^*} &= r_{[H^+]_{gel} \rightarrow [H^+]^*} - r_{[H^+]^* \rightarrow [H_R]^*} \\ &= k_{10} \cdot C_{[H^+]_{gel}} \cdot \frac{S^*}{S} \cdot \zeta_{[H^+]_{gel} \rightarrow [H^+]^*} \cdot \frac{V_r}{S} - k_{11} \cdot C_{[H^+]^*} \left[\frac{mol[H^+]^*}{m_c^2 \cdot s} \right] \end{aligned} \quad (\text{Eq. 2.41})$$

Chemical kinetics of the hydrogen radicals on the iron surface $[H_R]^o$:

Since hydrogen radical $[H_R]$ is at very unsteady state, two of them can combine shortly and become hydrogen molecules $[H_2]$ in the gel phase. The rate of consumption of hydrogen radicals $[H_R]$ can be expressed:

$$-r_{[H_R]^o \rightarrow [H_2]^o} = -\frac{dC_{[H_R]^o}}{dt} = k_{13} \cdot C_{[H_R]^o} \cdot C_{[H_R]^o} \left[\frac{mol[H_R]^o}{m_c^2 \cdot s} \right] \quad (\text{Eq. 2.42})$$

The production of hydrogen radicals because the hydrogen ions obtain electrons can be expressed:

$$r_{[H^+]^o \rightarrow [H_R]^o} = \frac{dC_{[H_R]^o}}{dt} = k_{12} \cdot C_{[H^+]^o} \cdot \zeta_{[H^+]^o \rightarrow [H_R]^o} \left[\frac{\text{mol}[H_R]^o}{m_c^2 \cdot s} \right] \quad (\text{Eq. 2.43})$$

The net chemical kinetics of the hydrogen radicals $[H_R]$ can be represented:

$$\begin{aligned} \Delta r_{[H_R]^o} &= -r_{[H_R]^o \rightarrow [H_2]^o} + r_{[H^+]^o \rightarrow [H_R]^o} \\ &= -k_{13} \cdot C_{[H_R]^o} \cdot C_{[H_R]^o} + k_{12} \cdot C_{[H^+]^o} \cdot \zeta_{[H^+]^o \rightarrow [H_R]^o} \left[\frac{\text{mol}[H_R]^o}{m_c^2 \cdot s} \right] \end{aligned} \quad (\text{Eq. 2.44})$$

Chemical kinetics of hydrogen molecules on the iron surface substrate $[H_2]^o$:

The rate of production of hydrogen molecules associated with the iron surface substrate on catalyst surface can be expressed:

$$r_{[H_R]^o \rightarrow [H_2]^o} = \frac{dC_{[H_2]^o}}{dt} = k_{13} \cdot C_{[H_R]^o} \cdot C_{[H_R]^o} \cdot \zeta_{[H_R]^o \rightarrow [H_2]^o} \left[\frac{\text{mol}[H_2]^o}{m_c^2 \cdot s} \right] \quad (\text{Eq. 2.45})$$

Once the hydrogen gas is adsorbed on the iron surface substrate, $[H_2]^o$ will migrate on the catalyst surface, and affixed with palladium surface as new species, surface hydrogen molecules $[H_2]^*$.

The rate of consumption $[H_2]^o$ can be expressed:

$$-r_{[H_2]^o \rightarrow [H_2]^*} = -\frac{dC_{[H_2]^o}}{dt} = k_{14} \cdot C_{[H_2]^o} \cdot \frac{S^*}{S} \left[\frac{\text{mol}[H_2]^o}{m_c^2 \cdot s} \right] \quad (\text{Eq. 2.46})$$

The net chemical kinetics of the hydrogen molecules associated with the iron surface substrate

$[H_2]^o$ can be represented:

$$\begin{aligned}
\Delta r_{[H_2]^o} &= r_{[H_R]^o \rightarrow [H_2]^o} - r_{[H_2]^o \rightarrow [H_2]^*} \\
&= k_{13} \cdot C_{[H_R]^o} \cdot C_{[H_R]^o} \cdot \zeta_{[H_R]^o \rightarrow [H_2]^o} - k_{14} \cdot C_{[H_2]^o} \cdot \frac{S^*}{S} \left[\frac{mol[H_2]^o}{m_c^2 \cdot s} \right]
\end{aligned} \tag{Eq.2.47}$$

Chemical kinetics of the hydrogen molecules on the palladium surface $[H_2]^*$:

The rate of production of hydrogen molecules associated with palladium surface $[H_2]^*$ due to the migration of $[H_2]^o$ can be expressed:

$$r_{[H_2]^o \rightarrow [H_2]^*} = \frac{dC_{[H_2]^*}}{dt} = k_{14} \cdot C_{[H_2]^o} \cdot \frac{S^*}{S} \cdot \zeta_{[H_2]^o \rightarrow [H_2]^*} \left[\frac{mol[H_2]^*}{m_c^2 \cdot s} \right] \tag{Eq. 2.48}$$

The rate of consumption of hydrogen molecules associated with sites $[H_2]^*$ due to the dissociation of hydrogen molecules around the palladium can be expressed:

$$-r_{[H_2]^* \rightarrow [H_R]^*} = -\frac{dC_{[H_2]^*}}{dt} = k_{18} \cdot C_{[H_2]^*} \cdot \frac{S^*}{S} \left[\frac{mol[H_2]^*}{m_c^2 \cdot s} \right] \tag{Eq. 2.49}$$

The net chemical kinetics of the hydrogen molecules associated with palladium surface $[H_2]^*$ can be represented:

$$\Delta r_{[H_2]^*} = r_{[H_2]^o \rightarrow [H_2]^*} - r_{[H_2]^* \rightarrow [H_R]^*} = k_{14} \cdot C_{[H_2]^o} \cdot \frac{S^*}{S} \cdot \zeta_{[H_2]^o \rightarrow [H_2]^*} - k_{18} \cdot C_{[H_2]^*} \cdot \frac{S^*}{S} \left[\frac{mol[H_2]^*}{m_c^2 \cdot s} \right] \tag{Eq. 2.50}$$

Chemical kinetics of the hydrogen radicals on the palladium surface $[H_R]^*$:

The rate of production of hydrogen radicals associated with sites $[H_R]^*$ due to the dissociation of hydrogen molecules can be expressed as:

$$r_{[H_2]^* \rightarrow [H_R]^*} = \frac{dC_{[H_R]^*}}{dt} = k_{18} \cdot C_{[H_2]^*} \cdot \frac{S^*}{S} \cdot \xi_{[H_2]^* \rightarrow [H_R]^*} \left[\frac{\text{mol}[H_R]^*}{m_c^2 \cdot s} \right] \quad (\text{Eq. 2.51})$$

The rate of consumption of hydrogen radicals associated with sites $[H_R]^*$ due to the first-step dechlorination can be expressed as:

$$-r_{[H_R]^* \rightarrow [R-HCl]^*} = -\frac{dC_{[H_R]^*}}{dt} = k_{23} \cdot C_{[R-HCl]^*} \cdot C_{[H_R]^*} \left[\frac{\text{mol}[H_R]^*}{m_c^2 \cdot s} \right] \quad (\text{Eq. 2.52})$$

The rate of consumption of hydrogen radicals associated with sites $[H_R]^*$ due to the second-step dechlorination can be expressed as:

$$-r_{[H_R]^* \rightarrow [HCl]^*} = -\frac{dC_{[H_R]^*}}{dt} = k_{24} \cdot C_{[R-HCl]^*} \cdot C_{[H_R]^*} \left[\frac{\text{mol}[H_R]^*}{m_c^2 \cdot s} \right] \quad (\text{Eq. 2.53})$$

$$r_{[H^+]^* \rightarrow [H_R]^*} = \frac{dC_{[H_R]^*}}{dt} = k_{11} \cdot C_{[H^+]^*} \cdot \xi_{[H^+]^* \rightarrow [H_R]^*} \left[\frac{\text{mol}[H_R]^*}{m_c^2 \cdot s} \right] \quad (\text{Eq. 2.54})$$

The net chemical kinetics of the hydrogen radicals associated with palladium surface $[H_R]^*$ can be represented:

$$\Delta r_{[H_R]^*} = r_{[H_2]^* \rightarrow [H_R]^*} - r_{[H_R]^* \rightarrow [R-HCl]^*} - r_{[H_R]^* \rightarrow [HCl]^*} + r_{[H^+]^* \rightarrow [H_R]^*} \quad (\text{Eq. 2.55})$$

$$\begin{aligned}
&= k_{11} \cdot C_{[H^+]}^* \cdot \xi_{[H^+]^* \rightarrow [H_R]^*} + k_{18} \cdot C_{[H_2]}^* \cdot \frac{S^*}{S} \cdot \xi_{[H_2]^* \rightarrow [H_R]^*} - k_{23} \cdot C_{[R-Cl]}^* \cdot C_{[H_R]^*} \\
&\quad - k_{24} \cdot C_{[R-HCl]}^* \cdot C_{[H_R]^*} \left[\frac{mol[H_R]^*}{m_c^2 \cdot s} \right]
\end{aligned}$$

Chemical kinetics of p-chlorophenol in the liquid phase of gel phase $[R-Cl]_{gel}$:

The p-chlorophenol in the gel phase can be adsorbed into the iron surface substrate on the catalyst surface. The rate of consumption of P-chlorophenol in the gel phase $[R-Cl]_{gel}$ because of adsorption of p-chlorophenol can be expressed:

$$-r_{[R-Cl]_{gel} \rightarrow [R-Cl]^o} = -\frac{dC_{[R-Cl]_{gel}}}{dt} = k_{19} \cdot C_{[R-Cl]_{gel}} \cdot \frac{S^o}{S} \left[\frac{mol[R-Cl]_{gel}}{m_g^3 \cdot s} \right] \quad (\text{Eq. 2.56})$$

The p-chlorophenol in the gel phase also can be directly adsorbed into the palladium surface on the catalyst surface. The process can be defined as the direct adsorption of p-chlorophenol. The rate of consumption of P-chlorophenol in gel phase $[R-Cl]_{gel}$ because of direct adsorption of p-chlorophenol can be expressed as:

$$-r_{[R-Cl]_{gel} \rightarrow [R-Cl]^*} = -\frac{dC_{[R-Cl]_{gel}}}{dt} = k_{21} \cdot C_{[R-Cl]_{gel}} \cdot \frac{S^*}{S} \left[\frac{mol[R-Cl]_{gel}}{m_g^3 \cdot s} \right] \quad (\text{Eq. 2.57})$$

The adsorption of p-chlorophenol is a reversible process, and thus the p-chlorophenol associated with iron surface substrate $[R-Cl]^o$ desorb the surface sites. The rate of production of p-chlorophenol because of deportation of $[R-Cl]^o$ can be expressed:

$$r_{[R-Cl]^o \rightarrow [R-Cl]_{gel}} = \frac{dC_{[R-Cl]_{gel}}}{dt} = k_{20} \cdot C_{[R-Cl]^o} \cdot \xi_{[R-Cl]^o \rightarrow [R-Cl]_{gel}} \cdot \frac{S}{V_g} \left[\frac{mol [R-Cl]_{gel}}{m_g^3 \cdot s} \right] \quad (\text{Eq. 2.58})$$

The net chemical kinetics for P-chlorophenol in the gel phase $[R-Cl]_{gel}$ can be expressed:

$$\begin{aligned} \Delta r_{[R-Cl]_{gel}} &= r_{[R-Cl]^o \rightarrow [R-Cl]_{gel}} - r_{[R-Cl]_{gel} \rightarrow [R-Cl]^o} - r_{[R-Cl]_{gel} \rightarrow [R-Cl]^*} \\ &= k_{19} \cdot C_{[R-Cl]^o} \cdot \xi_{[R-Cl]^o \rightarrow [R-Cl]_{gel}} \cdot \frac{S}{V_g} - k_{21} \cdot C_{[R-Cl]_{gel}} \cdot \frac{S^o}{S} - k_{20} \cdot C_{[R-Cl]_{gel}} \cdot \frac{S^*}{S} \left[\frac{mol [R-Cl]_{gel}}{m_g^3 \cdot s} \right] \end{aligned} \quad (\text{Eq. 2.59})$$

Chemical kinetics for p-chlorophenol on the iron surface $[R-Cl]^o$:

The rate of production of p-chlorophenol associated with the surface of the iron surface substrate $[R-Cl]^o$ due to the adsorption of p-chlorophenol onto the surface of the iron surface substrate on the catalyst surface can be expressed:

$$r_{[R-Cl]_{gel} \rightarrow [R-Cl]^o} = \frac{dC_{[R-Cl]^o}}{dt} = k_{19} \cdot C_{[R-Cl]_{gel}} \cdot \frac{S^o}{S} \cdot \xi_{[R-Cl]_{gel} \rightarrow [R-Cl]^o} \cdot \frac{V_g}{S} \left[\frac{mol [R-Cl]^o}{m_c^2 \cdot s} \right] \quad (\text{Eq. 2.60})$$

After occupying the iron surface substrate, this p-chlorophenol associated with iron surface substrate $[R-Cl]^o$ migrate to the palladium surface on the catalyst surface, and then they are associated with palladium surface. The consumption of p-chlorophenol associated with the surface of the iron surface substrate $[R-Cl]^o$ can be expressed:

$$-r_{[R-Cl]^o \rightarrow [R-Cl]^*} = -\frac{dC_{[R-Cl]^o}}{dt} = k_{21} \cdot C_{[R-Cl]^o} \cdot \frac{S^*}{S} \left[\frac{mol [R-Cl]^o}{m_c^2 \cdot s} \right] \quad (\text{Eq. 2.61})$$

The net chemical kinetics for the P-chlorophenol associate with the iron surface substrate $[R-Cl]^o$ can be expressed:

$$\Delta r_{[R-Cl]^o} = k_{19} \cdot C_{[R-Cl]_{gel}} \cdot \frac{S^o}{S} \cdot \xi_{[R-Cl]_{gel} \rightarrow [R-Cl]^o} \cdot \frac{V_g}{S} - k_{21} \cdot C_{[R-Cl]^o} \cdot \frac{S^*}{S} \left[\frac{mol[R-Cl]^o}{m_c^2 \cdot s} \right] \quad (\text{Eq.2.62})$$

Chemical kinetics for p-chlorophenol on the palladium surface $[R-Cl]^*$:

The rate of production of P-chlorophenol associating with palladium surface $[R-Cl]^*$ due to the activation of can be expressed:

$$r_{[R-Cl]^o \rightarrow [R-Cl]^*} = \frac{dC_{[R-Cl]^*}}{dt} = k_{21} \cdot C_{[R-Cl]^o} \cdot \frac{S^*}{S} \cdot \xi_{[R-Cl]^o \rightarrow [R-Cl]^*} \left[\frac{mol[R-Cl]^*}{m_c^2 \cdot s} \right] \quad (\text{Eq. 2.63})$$

The rate of production of P-chlorophenol associating with palladium surface $[R-Cl]^*$ because P-chlorophenol $[R-Cl]_{liquid}$ in the gel phase directly adsorbing onto the palladium surface on catalyst surface can be expressed:

$$r_{[R-Cl]_{gel} \rightarrow [R-Cl]^*} = \frac{dC_{[R-Cl]^*}}{dt} = k_{22} \cdot C_{[R-Cl]_{gel}} \cdot \frac{S^*}{S} \cdot \xi_{[R-Cl]_{gel} \rightarrow [R-Cl]^*} \cdot \frac{V_g}{S} \left[\frac{mol[R-Cl]^*}{m_c^2 \cdot s} \right] \quad (\text{Eq. 2.64})$$

When he $[R-Cl]^*$ reacts with $[H_R]^*$, the dechlorination occurs on the catalyst surface. The whole dechlorination occurs in two steps, the first one is that the production of intermediate species $[R-HCl]^*$. The rate of consumption of P-chlorophenol associating with palladium surface $[R-Cl]^*$ can be expressed as:

$$-r_{[R-Cl]^* \rightarrow [R-HCl]^*} = -\frac{dC_{[R-Cl]^*}}{dt} = k_{23} \cdot C_{[R-Cl]^*} \cdot C_{[H_R]^*} \left[\frac{mol[R-Cl]^*}{m_c^2 \cdot s} \right] \quad (\text{Eq. 2.65})$$

The net chemical kinetics for P-chlorophenol occupying palladium surface $[R-Cl]^*$ can be expressed:

$$\begin{aligned} \Delta r_{[R-Cl]^*} &= r_{[R-Cl]^o \rightarrow [R-Cl]^*} + r_{[R-Cl]_{gel} \rightarrow [R-Cl]^*} - r_{[R-Cl]^* \rightarrow [R-HCl]^*} \\ &= k_{21} \cdot C_{[R-Cl]^o} \cdot \frac{S^*}{S} \cdot \xi_{[R-Cl]^o \rightarrow [R-Cl]^*} + k_{22} \cdot C_{[R-Cl]_{gel}} \cdot \frac{S^*}{S} \cdot \xi_{[R-Cl]_{gel} \rightarrow [R-Cl]^*} \cdot \frac{V_g}{S} \\ &\quad - k_{23} \cdot C_{[R-Cl]^*} \cdot C_{[H_R]^*} \left[\frac{mol[R-Cl]^*}{m_c^2 \cdot s} \right] \end{aligned} \quad (\text{Eq. 2.66})$$

Chemical kinetics of intermediate species $[R-HCl]^*$:

As mentioned before, the intermediate species $[R-HCl]^*$ is produced during the first-step dechlorination. The rate of production of intermediate species $[R-HCl]^*$ can be expressed:

$$r_{[R-Cl]^* \rightarrow [R-HCl]^*} = \frac{dC_{[R-HCl]^*}}{dt} = k_{23} \cdot C_{[R-Cl]^*} \cdot C_{[H_R]^*} \cdot \xi_{[R-Cl]^* \rightarrow [R-HCl]^*} \left[\frac{mol[R-HCl]^*}{m_c^2 \cdot s} \right] \quad (\text{Eq. 2.67})$$

The intermediate species $[R-HCl]^*$ continue to react with hydrogen radicals associating with palladium surface $[H_R]^*$, which can be defined as the second step of dechlorination. The rate of consumption of the intermediate species $[R-HCl]^*$ can be expressed as:

$$-r_{[R-HCl]^* \rightarrow [R]^*} = -\frac{dC_{[R-HCl]^*}}{dt} = k_{24} \cdot C_{[R-HCl]^*} \cdot C_{[H_R]^*} \left[\frac{mol[R-HCl]^*}{m_c^2 \cdot s} \right] \quad (\text{Eq. 2.68})$$

The net chemical kinetics for intermediate species $[R-HCl]^*$ can be represented:

$$\Delta r_{[R-HCl]^*} = r_{[R-Cl]^* \rightarrow [R-HCl]^*} - r_{[R-HCl]^* \rightarrow [R]^*} \quad (\text{Eq. 2.69})$$

$$= k_{23} \cdot C_{[R-Cl]^*} \cdot C_{[H_R]^*} \cdot \xi_{[R-Cl]^* \rightarrow [R-HCl]^*} - k_{24} \cdot C_{[R-HCl]^*} \cdot C_{[H_R]^*} \left[\frac{mol[R-HCl]^*}{m_c^2 \cdot s} \right]$$

Chemical kinetics of the phenol on the palladium surface $[R]^*$:

During the second-step dechlorination, the intermediates species $[R-HCl]^*$ react with hydrogen radicals associating with palladium surface $[H_R]^*$, producing the final product: the phenol associated with palladium surface $[R]^*$ and hydrogen chloride associated with palladium surface $[HCl]^*$. The rate of production of phenol associated with palladium surface $[R]^*$ due to the second-step reaction of dechlorination can be expressed:

$$r_{[R-HCl]^* \rightarrow [R]^*} = \frac{dC_{[R]^*}}{dt} = k_{24} \cdot C_{[R-HCl]^*} \cdot C_{[H_R]^*} \cdot \xi_{[R-HCl]^* \rightarrow [R]^*} \left[\frac{mol[R]^*}{m_c^2 \cdot s} \right] \quad (\text{Eq. 2.70})$$

The phenol associated with palladium surface $[R]^*$ eventually desorb from palladium surface. The consumption of phenol associated with palladium surface $[R]^*$ can be expressed:

$$-r_{[R]^* \rightarrow [R]_{liquid}} = -\frac{dC_{[R]^*}}{dt} = k_{25} \cdot C_{[R]^*} \left[\frac{mol[R]^*}{m_c^2 \cdot s} \right]$$

(Eq. 2.71)

The net chemical kinetics of the phenol associated with palladium surface $[R]^*$:

$$\Delta r_{[R]^*} = r_{[R-HCl]^* \rightarrow [R]^*} - r_{[R]^* \rightarrow [R]_{gel}} = k_{24} \cdot C_{[R-HCl]^*} \cdot C_{[H_R]^*} \cdot \xi_{[R-HCl]^* \rightarrow [R]^*} - k_{25} \cdot C_{[R]^*} \left[\frac{mol[R]^*}{m_c^2 \cdot s} \right] \quad (\text{Eq. 2.72})$$

Chemical kinetics of the phenol in the liquid phase of gel phase $[R]_{gel}$:

The rate of production of phenol in the gel phase $[R]_{gel}$ due to the desorption of $[R]^*$ can be expressed:

$$r_{[R]^* \rightarrow [R]_{gel}} = k_{25} \cdot C_{[R]^*} \cdot \xi_{[R]^* \rightarrow [R]_{gel}} \cdot \frac{S}{V_g} \left[\frac{mol[R]_{gel}}{m_g^3 \cdot s} \right] \quad (\text{Eq. 2.73})$$

The total change of concentration for the phenol in the gel phase $[R]_{gel}$:

$$\Delta r_{[R]_{liquid}} = r_{[R]^* \rightarrow [R]_{gel}} = k_{25} \cdot C_{[R]^*} \cdot \xi_{[R]^* \rightarrow [R]_{gel}} \cdot \frac{S}{V_g} \left[\frac{mol[R]_{gel}}{m_g^3 \cdot s} \right] \quad (\text{Eq. 2.74})$$

Chemical kinetics of the iron surface S^o :

Since iron surface has been occupied by hydrogen ions, so the adsorption can be treated as 'consumption of surface of iron surface substrate' and the rate of consumption can be expressed by:

$$-r_{S^o([H^+]_{gel} \rightarrow [H^+]^o)} = -\frac{d(S^o/S)}{dt} = k_8 \cdot C_{[H^+]_{gel}} \cdot \frac{S^o}{S} \cdot \frac{V_g}{S} \cdot \eta_{S^o[H^+]^o} \left[\frac{m_{S^o}^2}{m_c^2 \cdot s} \right] \quad (\text{Eq. 2.75})$$

The hydrogen molecules associated with iron surface substrate leaves the iron surface substrate and occupy the palladium surface. Therefore, the rate of release of the iron surface can be expressed:

$$r_{S^o([H_2]^o \rightarrow [H_2]^p)} = \frac{d(S^o/S)}{dt} = k_{14} \cdot C_{[H_2]^o} \cdot \frac{S^*}{S} \cdot \eta_{S^o[H_2]^o} \left[\frac{m_{S^o}^2}{m_c^2 \cdot s} \right] \quad (\text{Eq. 2.76})$$

$$r_{S^o([H_R]^o \rightarrow [H_2]^o)} = \frac{d(S^o/S)}{dt} = k_{13} \cdot C_{[H_R]^o} \cdot \eta_{S^o[H_R]^o} \left[\frac{m_{S^o}^2}{m_c^2 \cdot s} \right] \quad (\text{Eq. 2.77})$$

Since the iron surface substrate has been occupied by p-chlorophenol molecule, so the adsorption can be treated as 'consumption of the iron surface substrate' and the rate of consumption can be express:

$$-r_{S^o([R-Cl]_{gel} \rightarrow [R-Cl]^o)} = -\frac{d(S^o / S)}{dt} = k_{19} \cdot C_{[R-Cl]_{gel}} \cdot \frac{S^o}{S} \cdot \frac{V_g}{S} \cdot \xi_{[R-Cl]_{gel} \rightarrow [R-Cl]^o} \cdot \eta_{S^o[R-Cl]^o} \left[\frac{m_{S^o}^2}{m_c^2 \cdot s} \right] \quad (\text{Eq. 2.78})$$

The p-chlorophenol molecules associated with the iron surface substrate migrate from the iron surface substrate to the palladium surface. Therefore, the rate of production of the iron surface substrate can be expressed:

$$r_{S^o([R-Cl]^o \rightarrow [R-Cl]^*)} = \frac{d(S^o / S)}{dt} = k_{21} \cdot C_{[R-Cl]^o} \cdot \frac{S^*}{S} \cdot \eta_{S^o[R-Cl]^o} \left[\frac{m_{S^o}^2}{m_c^2 \cdot s} \right] \quad (\text{Eq. 2.79})$$

The net chemical kinetics for the iron surface substrate S^o can be represented:

$$\Delta r_{S^o} = -k_8 \cdot C_{[H^+]_{gel}} \cdot \frac{S^o}{S} \cdot \frac{V_g}{S} \cdot \eta_{S^o[H^+]^o} + k_{21} \cdot C_{[R-Cl]^o} \cdot \frac{S^*}{S} \cdot \eta_{S^o[R-Cl]^o} + k_{14} \cdot C_{[H_2]^o} \cdot \frac{S^*}{S} \cdot \eta_{S^o[H_2]^o} \quad (\text{Eq. 2.80})$$

$$-k_{19} \cdot C_{[R-Cl]_{gel}} \cdot \frac{S^o}{S} \cdot \frac{V_g}{S} \cdot \xi_{[R-Cl]_{gel} \rightarrow [R-Cl]^o} \cdot \eta_{S^o[R-Cl]^o}$$

Chemical kinetics of the palladium surface S^* :

The $[H_2]^o$ leaves the iron surface substrate and occupy the palladium surface. Therefore, the process can be treated as 'consumption of the palladium surface and the rate of consumption of palladium surface can be expressed by:

$$-r_{S^*([H_2]^o \rightarrow [H_2]^*)} = -\frac{d(S^*/S)}{dt} = k_{14} \cdot C_{[H_2]^o} \cdot \frac{S^*}{S} \cdot \xi_{[H_2]^o \rightarrow [H_2]^*} \cdot \eta_{S^*[H_2]^*} \left[\frac{m_{S^*}^2}{m_c^2 \cdot s} \right] \quad (\text{Eq. 2.81})$$

The hydrogen ions in the gel phase occupy the palladium surface. Therefore, the process can be treated as ‘consumption of the palladium surface and the rate of consumption of palladium surface can be expressed by:

$$-r_{S^*([H^+]_{gel} \rightarrow [H^+]^*)} = -\frac{d(S^*/S)}{dt} = k_{10} \cdot C_{[H^+]_{gel}} \cdot \frac{S^*}{S} \cdot \frac{V_g}{S} \cdot \xi_{[H^+]_{gel} \rightarrow [H^+]^*} \cdot \eta_{S^*[H^+]^*} \left[\frac{m_{S^*}^2}{m_c^2 \cdot s} \right] \quad (\text{Eq. 2.82})$$

Since the palladium surface have been occupied by p-chlorophenol molecule directly, the direct adsorption can be treated as ‘consumption of the palladium surface and the rate of consumption can be expressed by

$$-r_{S^*([R-Cl]_{gel} \rightarrow [R-Cl]^*)} = -\frac{d(S^*/S)}{dt} = k_{22} \cdot C_{[R-Cl]_{gel}} \cdot \frac{S^*}{S} \cdot \frac{V_g}{S} \cdot \xi_{[R-Cl]_{gel} \rightarrow [R-Cl]^*} \cdot \eta_{S^*[R-Cl]^*} \left[\frac{m_{S^*}^2}{m_c^2 \cdot s} \right] \quad (\text{Eq. 2.83})$$

The p-chlorophenol molecules associated with the iron surface substrate moves to the palladium surface. The rate of consumption of palladium surface can be expressed by:

$$-r_{S^*([R-Cl]^o \rightarrow [R-Cl]^*)} = -\frac{d(S^*/S)}{dt} = k_{21} \cdot C_{[R-Cl]^o} \cdot \frac{S^*}{S} \cdot \xi_{[R-Cl]^o \rightarrow [R-Cl]^*} \cdot \eta_{S^*[R-Cl]^*} \left[\frac{m_{S^*}^2}{m_c^2 \cdot s} \right] \quad (\text{Eq.2.84})$$

The $[H_2]^*$ leaves the iron surface substrate and occupy the palladium surface. Therefore, the rate of consumption of palladium surface can be expressed by

$$-r_{S^*([H_2]^* \rightarrow [H_R]^*)} = -\frac{d(S^*/S)}{dt} = k_{18} \cdot C_{[H_2]^*} \cdot \eta_{S^*[H_R]^*} \left[\frac{m_{S^*}^2}{m_c^2 \cdot s} \right] \quad (\text{Eq. 2.85})$$

The rate of production of the catalyst-surface containing palladium surface due to desorption of species $[R]^*$ can be represented:

$$r_{S^*([R]^* \rightarrow [R]_{gel})} = \frac{d(S^* / S)}{dt} = k_{25} \cdot C_{[R]^*} \cdot \eta_{S^*[R]^*} \left[\frac{m_{S^*}^2}{m_c^2 \cdot S} \right] \quad (\text{Eq. 2.86})$$

The rate of production of the catalyst-surface containing palladium surface due to desorption of species $[HCl]^*$ can be represented:

$$r_{S^*([HCl]^* \rightarrow [HCl]_{gel})} = \frac{d(S^* / S)}{dt} = k_{26} \cdot C_{[HCl]^*} \cdot \eta_{S^*[HCl]^*} \left[\frac{m_{S^*}^2}{m_c^2 \cdot S} \right] \quad (\text{Eq. 2.87})$$

The net chemical kinetics for the iron surface substrate S^* can be represented:

$$\begin{aligned} \therefore \Delta r_{S^*} = & -k_{10} \cdot C_{[H^+]_{gel}} \cdot \frac{S^*}{S} \cdot \frac{V_g}{S_c} \cdot \xi_{[H^+]_{gel} \rightarrow [H^+]} \cdot \eta_{S^*[H^+]} - k_{22} \cdot C_{[R-Cl]_{gel}} \cdot \frac{S^*}{S} \cdot \frac{V_g}{S} \cdot \xi_{[R-Cl]_{gel} \rightarrow [R-Cl]} \cdot \eta_{S^*[R-Cl]} \\ & - k_{14} \cdot C_{[H_2]^o} \cdot \frac{S^*}{S} \cdot \xi_{[H_2]^o \rightarrow [H_2]} \cdot \eta_{S^*[H_2]} - k_{21} \cdot C_{[R-Cl]^o} \cdot \frac{S^*}{S} \cdot \xi_{[R-Cl]^o \rightarrow [R-Cl]} \cdot \eta_{S^*[R-Cl]} - k_{18} \cdot C_{[H_2]^*} \cdot \eta_{S^*[H_2]^*} \\ & + k_{25} \cdot C_{[R]^*} \cdot \eta_{S^*[R]^*} + k_{26} \cdot C_{[HCl]^*} \cdot \eta_{S^*[HCl]^*} \left[\frac{m_{S^*}^2}{m_c^2 \cdot S} \right] \end{aligned} \quad (\text{Eq. 2.88})$$

Chapter 3 Mathematical Model for Mass Balance

3.1 Mass Balance Equations in the Main Fluid and Gel Phase

To calculate the mass transfer of materials, including reactants p-chlorophenol and the products phenol in microscale reactor, it is necessary to build up a useful and easily calculated mathematical model. To realize this object, reasonable assumptions, differential equations, boundary and inlet conditions, any other type of correlation or simplification should be used. The appreciate variables for the model are the diffusion coefficient, the convection coefficient, reaction rate etc. To simplify the mathematical model, a simple micro-reactor can be constructed as three parallel plates as shown in the illustration section. Several appreciate assumption should be created: 1) the diffusion of p-chlorophenol is two-dimensional (along x, y-direction) and fully developed. 2) The diffusion coefficients at the gel phase and gel part are both constant. 3) The whole reaction process is steady state. 4) The p-chlorophenol is unidirectional laminar flow in the gel phase. 5) Assume there is no temperature change during the reaction. 6) The total amount of catalyst is constant.

A mass transfer equation is of the form: Rate of mass into control Volume-Rate of mass out of control volume. The rate of accumulation of control volume. In the gel phase of the control volume, the diffusion occurs in the flow direction(x) and convections in the vertical direction (y). The inputs and the outputs of mass are by convective flow in the x-direction or by diffusion in both y and x directions. The accumulation represents the net production of the inputs and the outputs, which can be assumed as zero because the process is in the steady state. According to the final solution of the velocity of p-chlorophenol, the pressure difference between the entrance and end of the reactor, the viscosity and the distance along y-direction from the top wall of reactor affect the

velocity of p-chlorophenol. However, the pressure difference and the viscosity are constant. The velocity of p-chlorophenol changes along the y-direction only depends on the distance along the y-direction. Based on the final solution, the velocity of p-chlorophenol reaches the maximum at the center of the reactor ($y = d_1$). In addition, the velocity along x-direction decreases to the zero when p-chlorophenol reaches the interface between the main fluid and catalyst part ($y = d_2$). Therefore, without velocity, the convection cannot occur in the catalyst part. The details about developing mass transfer equations for p-chlorophenol in the microscale-based reactor can be in Appendix B.

In the main fluid, when the p-chlorophenol enters the microscale-based reactor, it diffuses immediately due to the difference of concentration. At the same time, since p-chlorophenol flows with a certain velocity along the x-direction, and thus the convection along x-direction also happens in the main fluid. Therefore, in a two-dimensional formulation, at steady state, the partial differential equation of p-chlorophenol mass transfer in main fluid for a two-parallel plate reactor is governed by:

$$(u_x)_{[R-Cl]_{fluid}} \cdot \frac{\partial C_{[R-Cl]_{fluid}}}{\partial x} + D_1 \frac{\partial^2 C_{[R-Cl]_{fluid}}}{\partial x^2} + D_1 \frac{\partial^2 C_{[R-Cl]_{fluid}}}{\partial y^2} = 0 \quad (\text{Eq. 3.1})$$

Apart from the mass balance equations concerned with the mass transfer of p-chlorophenol, several proper boundary conditions should be established as well. When p-chlorophenol enters the micro-reactor at $x = 0$ and $0 < y < d_1$, the concentration of p-chlorophenol is uniform and constant and is

equal to the inlet concentration of p-chlorophenol. The inlet concentration can be measured in the experiment. The first boundary condition can be expressed by:

$$\text{BC-1: } x = 0, \quad d_1 < y < d_2 \quad C_{[R-Cl]_{fluid}} = C_{[R-Cl]_{inlet}} \quad (\text{Eq. 3.2})$$

When p-chlorophenol leaves the microscale-based reactor at $x = L$ and $0 < y < d_1$, at the end of the reactor. It is assumed that there is no flux of p-chlorophenol in gel phase along the x-direction.

The second boundary condition can be expressed by:

$$\text{BC-2: } x = L, \quad d_1 < y < d_2 \quad \frac{dC_{[R-Cl]_{fluid}}}{dx} = 0 \quad (\text{Eq. 3.3})$$

From the simple illustration, the top of the microscale-based reactor ($y = 0$) is a closed wall, so there is no flux of p-chlorophenol at $0 < x < L, y = 0$ the third boundary condition can be expressed by:

$$\text{BC-3: } 0 < x < L, \quad y = d_1 \quad \frac{dC_{[R-Cl]_{fluid}}}{dy} = 0 \quad (\text{Eq. 3.4})$$

When the p-chlorophenol reaches the interface between the main fluid and gel part at $0 < x < L, y = d_1$, the flux of p-chlorophenol in the main fluid is equal to the flux of p-chlorophenol in gel part. In addition, the value of the concentration of p-chlorophenol in the gel phase and in the gel part is the same as well. Therefore, the two boundary conditions can be expressed by:

BC-4:

$$0 < x < L, \quad y = d_1 \quad D_1 A_1 \frac{dC_{[R-Cl]_{fluid}}}{dy} = D_2 A_2 \frac{dC_{[R-Cl]_{gel}}}{dy} \quad (\text{Eq. 3.5})$$

$$D_1 \frac{dC_{[R-Cl]_{fluid}}}{dy} = D_2 \frac{A_2}{A_1} \frac{dC_{[R-Cl]_{gel}}}{dy}$$

In the gel part, since the velocity of p-chlorophenol decreased to the zero, there is only diffusion but convection. The p-chlorophenol diffuses along x and y-direction because of the difference of concentration. However, since there is no influence of convection, the diffusion coefficient of p-chlorophenol in gel part supposedly different from in main fluid. In addition, the dechlorination occurs in the gel part, which leads the generation of p-chlorophenol to happen in the gel part. Therefore, the total mass transfer of p-chlorophenol in gel part can be expressed by:

$$D_2 \frac{\partial^2 C_{[R-Cl]_{gel}}}{\partial x^2} + D_2 \frac{\partial^2 C_{[R-Cl]_{gel}}}{\partial y^2} + \Delta r_{[R-Cl]_{gel}} = 0 \quad (\text{Eq. 3.6})$$

$$D_2 \frac{\partial^2 [C_{R-Cl}]_{gel}}{\partial x^2} + D_2 \frac{\partial^2 [C_{R-Cl}]_{gel}}{\partial y^2} - k_{21} \cdot C_{[R-Cl]_{gel}} \cdot \frac{S^o}{S} - k_{20} \cdot C_{[R-Cl]_{gel}} \cdot \frac{S^*}{S} = 0 \quad (\text{Eq. 3.7})$$

$$\text{BC-1} : 0 < x < L, \quad y = d_1, \quad [C_{R-Cl}]_{fluid} = [C_{R-Cl}]_{gel} \quad (\text{Eq. 3.8})$$

In the gel part, the one closed wall is at $x = 0, d_1 < y < d_2$, so the concentration of p-chlorophenol is equal to zero and the boundary condition can be expressed by:

$$\text{BC-2} : x = 0, \quad d_1 < y < d_2 \quad \frac{dC_{[R-Cl]_{gel}}}{dx} = 0 \quad (\text{Eq. 3.9})$$

Similarly, the other closed wall is at $x = L, d_1 < y < d_2$, so the concentration of p-chlorophenol is equal to zero and the boundary condition can be expressed by:

$$\text{BC-3} : x = L, \quad d_1 < y < d_2 \quad \frac{dC_{[R-Cl]_{gel}}}{dx} = 0 \quad (\text{Eq. 3.10})$$

At the bottom of the microscale-based reactor, there is also a closed wall at $0 < x < L, y = d_2$, so the concentration of p-chlorophenol is equal to zero and the boundary condition can be expressed by:

$$\text{BC-4: } 0 < x < L, \quad y = d_2 \quad \frac{dC_{[R-Cl]_{gel}}}{dy} = 0 \quad (\text{Eq. 3.11})$$

The final products generate around the palladium surface. The process of developing mass transfer equation for $[R]$ is explored in the Appendix O. Since the net chemical kinetics for $[R]$ is expressed as Eq 2.71, the final mass transfer equation for $[R]$ can be represented as Eq.3.54.

$$D_2 \frac{\partial^2 C_{[R]_{gel}}}{\partial x^2} + D_2 \frac{\partial^2 C_{[R]_{gel}}}{\partial y^2} + \Delta r_{[R]_{gel}} = 0 \quad (\text{Eq. 3.12})$$

$$D_2 \frac{\partial^2 C_{[R]_{gel}}}{\partial x^2} + D_2 \frac{\partial^2 C_{[R]_{gel}}}{\partial y^2} + k_{25} \cdot C_{[R]^*} \cdot \xi_{[R]^* \rightarrow [R]_{gel}} \cdot \frac{S}{V_g} = 0 \quad (\text{Eq. 3.13})$$

When the phenol enters the gel phase, it diffuses immediately to the main fluid due to the difference of concentration. At the same time, since phenol flows out the reactor with a certain velocity along the x-direction, and thus the convection of phenol happens in the main fluid. Therefore, in a two-dimensional formulation, at steady state, the partial differential equation of phenol mass transfer in main fluid for a two-parallel plate reactor is governed by:

$$(u_x)_{[R]_{fluid}} \frac{\partial C_{[R]_{fluid}}}{\partial x} + D_1 \frac{\partial^2 C_{[R]_{fluid}}}{\partial x^2} + D_1 \frac{\partial^2 C_{[R]_{fluid}}}{\partial y^2} = 0 \quad (\text{Eq. 3.14})$$

When finishing the mass transfer of volumetric p-chlorophenol in the gel phase, the next part should focus on the solid Fe/Pd catalyst surface where a series of reactions occur. Since the diffusion on the catalyst is different from the ordinary diffusion, the terms representing the diffusion in the mass balance equation for surface species should be canceled. Therefore, the only term in the final mass balance equations is net chemical kinetics that can be obtained in the previous chapter. Table 3.1 shows final mass balance equations for all surface species. The more

detail about these mass balance equations for species on the catalyst surface is indicated in AppendixD.

Table3.1 The final mass balance equations for species on the catalyst surface

Mass balance equations for hydrogen molecules on the iron surface
$k_{13} \cdot C_{[H_R]^o} \cdot C_{[H_R]^o} \cdot \xi_{[H_R]^o \rightarrow [H_2]^o} - k_{15} \cdot C_{[H_2]^o} \cdot \xi_{[H_2]^o \rightarrow [H_2]_{gel}} \cdot \frac{S}{V_g} - k_{14} \cdot C_{[H_2]^o} \cdot \frac{S^*}{S} = 0$
Mass balance equations for hydrogen molecules on the palladium surface
$k_{14} \cdot C_{[H_2]^o} \cdot \frac{S^*}{S} \cdot \xi_{[H_2]^o \rightarrow [H_2]^*} + k_{17} \cdot C_{[H_2]_{gel}} \cdot \frac{S^*}{S} \cdot \xi_{[H_2]_{gel} \rightarrow [H_2]^*} \cdot \frac{V_g}{S} - k_{18} \cdot C_{[H_2]^*} \cdot \frac{S^*}{S} = 0$
Mass balance equations for hydrogen radicals on the palladium surface
$k_{11} \cdot C_{[H^+]^*} \cdot \xi_{[H^+]^* \rightarrow [H_R]^*} + k_{18} \cdot C_{[H_2]^*} \cdot \frac{S^*}{S} \cdot \xi_{[H_2]^* \rightarrow [H_R]^*} - k_{23} \cdot C_{[R-Cl]^*} \cdot C_{[H_R]^*} - k_{24} \cdot C_{[R-HCl]^*} \cdot C_{[H_R]^*} = 0$
Mass balance equations for p-chlorophenol on the iron surface
$k_{19} \cdot C_{[R-Cl]^o} \cdot \frac{S^o}{S} \cdot \xi_{R-Cl \rightarrow [R-Cl]^o} \cdot \frac{V_g}{S} - k_{21} \cdot C_{[R-Cl]^o} \cdot \frac{S^*}{S} - k_{20} \cdot C_{[R-Cl]^o} = 0$
Mass balance equations for p-chlorophenol on the palladium surface
$k_{21} \cdot C_{[R-Cl]^o} \cdot \frac{S^*}{S} \cdot \xi_{[R-Cl]^o \rightarrow [R-Cl]^*} + k_{22} \cdot C_{[R-Cl]_{gel}} \cdot \frac{S^*}{S} \cdot \xi_{[R-Cl]_{gel} \rightarrow [R-Cl]^*} \cdot \frac{V_g}{S} - k_{23} \cdot C_{[R-Cl]^*} \cdot C_{[H_R]^*} = 0$
Mass balance equations for intermediate species on the palladium surface
$k_{23} \cdot C_{[R-Cl]^*} \cdot C_{[H_R]^*} \cdot \xi_{[R-Cl]^* \rightarrow [R-HCl]^*} - k_{24} \cdot C_{[R-HCl]^*} \cdot C_{[H_R]^*} = 0$
Mass balance equations for phenol on the palladium surface
$k_{24} \cdot C_{[R-HCl]^*} \cdot C_{[H_R]^*} \cdot \xi_{[R-HCl]^* \rightarrow [R]^*} - k_{25} \cdot C_{[R]^*} = 0$

Chapter 4 Numerical Simulation of the Mass Balance

After establishing a mathematical model for mass transfer for p-chlorophenol, it is necessary to simulate the model by COMSOL software to validate the mathematical model. The screen image of the model in COMSOL software is indicated in appendix E. Apart from the p-chlorophenol and phenol in the main fluid and in the gel phase, all chemicals will be without the diffusion and convection in the mass balance equations, because surface diffusion is much slower than the ordinary diffusion, which can be ignored. In other words, the net chemical kinetics for chemicals that are produced on the catalyst surface can represent the mass balance for them. However, as far as p-chlorophenol and phenol concerned, they will diffuse in the main fluid and gel phase and they are involved in the dechlorinated reaction in the gel phase. In the model of the simulation for the p-chlorophenol mass transfer, the inlet concentration of p-chlorophenol is assumed to be 1 and the length of the reactor 15mm.

Figure 3.1 is the concentration profile of p-chlorophenol and phenol in the main fluid, which indicates that the concentration of p-chlorophenol gradually decreases due to the diffusion in the main fluid. Since p-chlorophenol fluid reaches a steady state in the reactor, its' concentration will be the function with the length of the reactor rather than with time. Additionally, figure 3.1 proves the boundary conditions for the mass transfer of p-chlorophenol in the reactor because the flux of p-chlorophenol is zero at the end of the reactor($x=15\text{mm}$). The slope of the curve in the figure decreases because the reduction of the concentration of p-chlorophenol leads to the decrease of the reaction rate. Figure 3.3 and 3.4 demonstrate the concentration profile of p-

chlorophenol and phenol at different locations in the liquid phase of the gel phase. The production phenol is generated in the gel phase due to the dechlorinated reaction and diffuses to the main fluid from the gel phase. It is also beneficial to explore the concentration profile of p-chlorophenol and phenol concentration profile in the y-direction at different x positions, which is significant to analyze the mass conversation of the reaction process. Figure 3.4 and figure 3.5 demonstrate the concentration of p-chlorophenol and phenol in the y0direction at x=5mm. Both figure 3.4 and figure 3.5 match the predicted mathematical model and boundary conditions, which demonstrates that there is no flux at the top and bottom of the reactor. The figure 3.6 and figure 3.7 indicates the similar distribution concentration profile of p-chlorophenol and phenol because the diffusion occurs in the main fluid and reactions happens in the gel phase in the y-direction although they are at different x positions. The total concentration of p-chlorophenol and phenol at the end of the reactor equals the inlet concentration of p-chlorophenol, which explains the mass balance in the reaction process

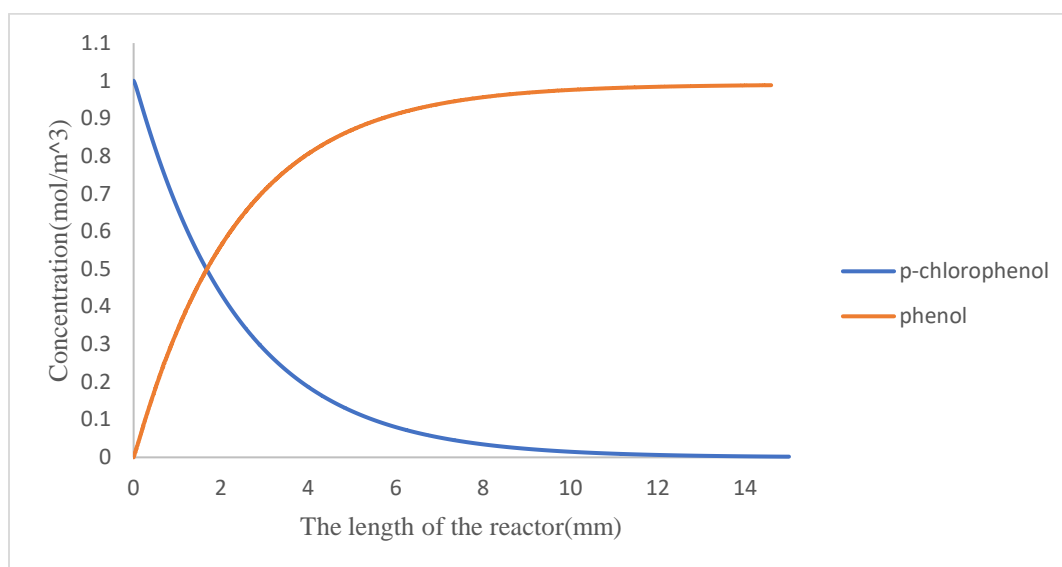


Figure 3.1 The concentration of p-chlorophenol and phenol in the x-direction in the main fluid

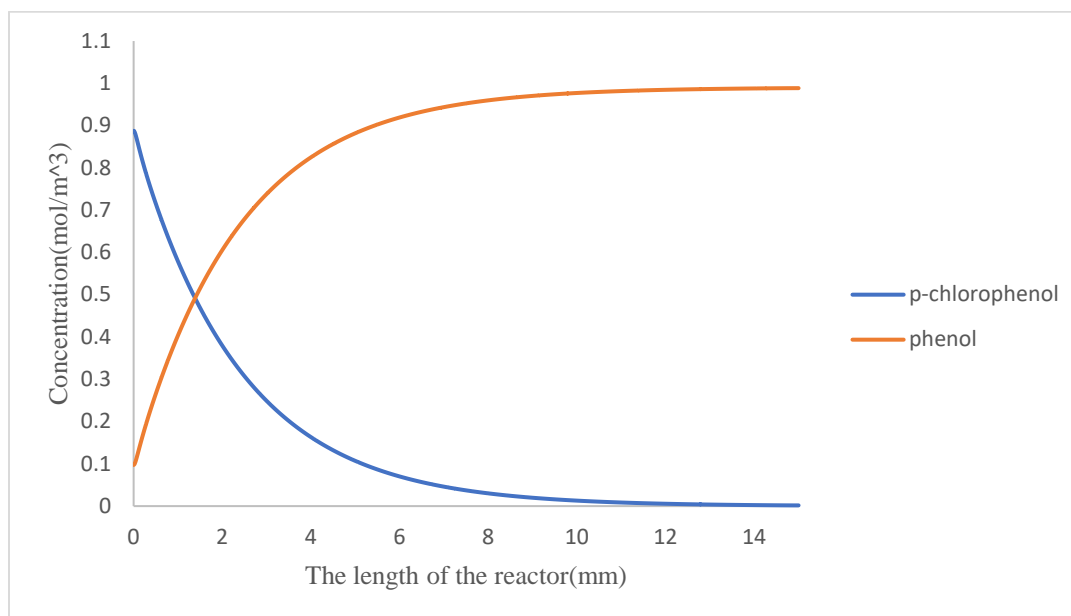


Figure 3.2 The concentration of p-chlorophenol and phenol in the x-direction at the middle of the gel phase

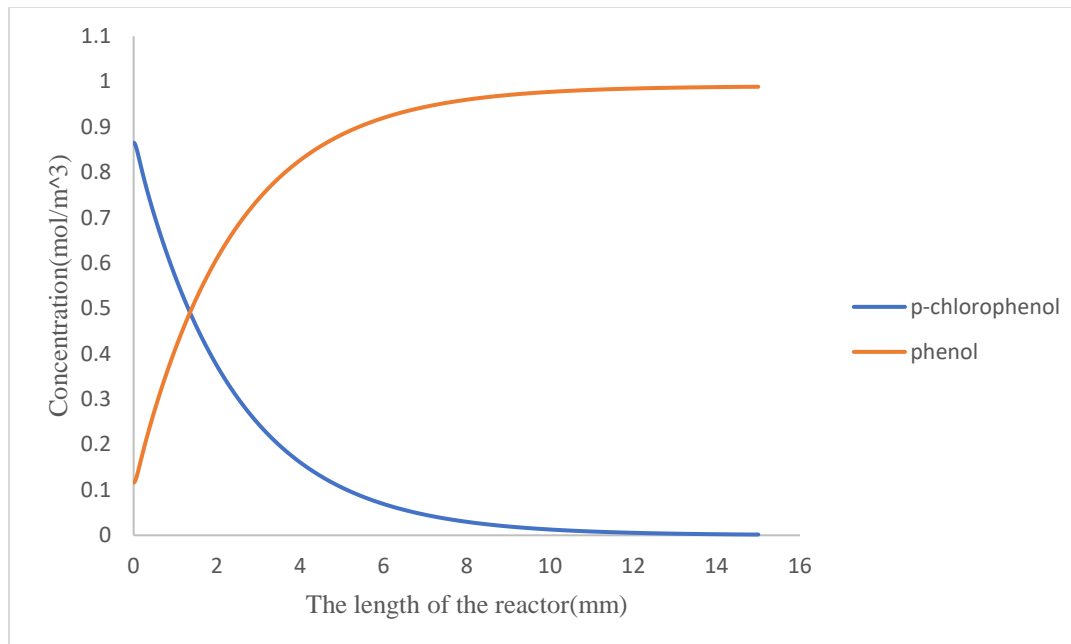


Figure 3.3 The concentration of p-chlorophenol and phenol in the x-direction at the bottom of the gel phase

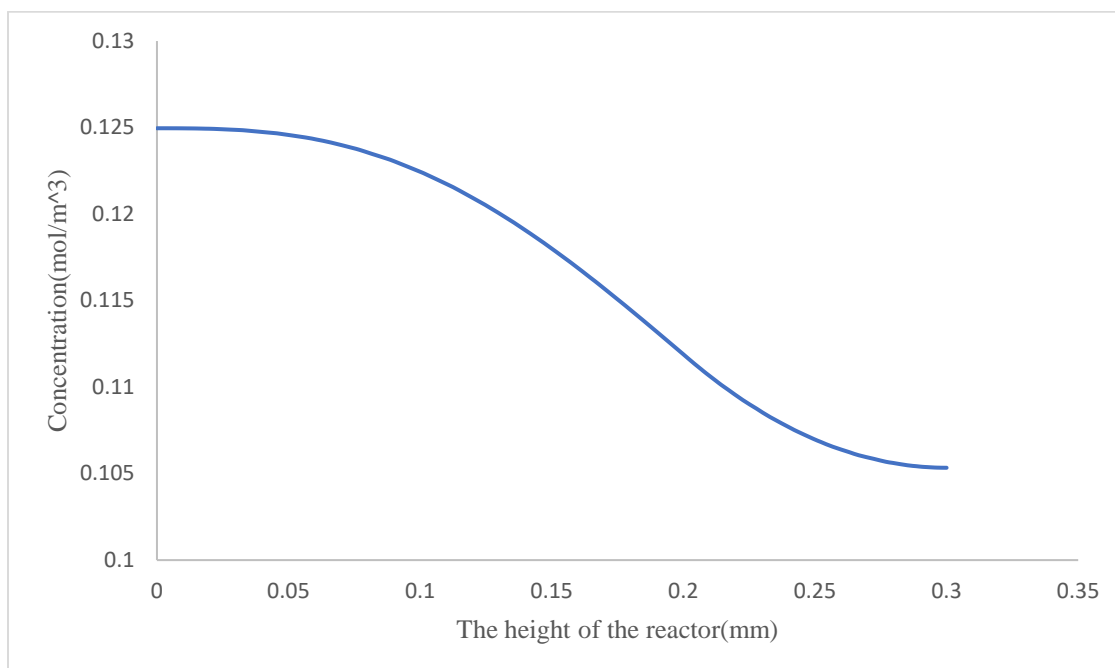


Figure 3.4 The concentration of p-chlorophenol in the y-direction at x=5mm

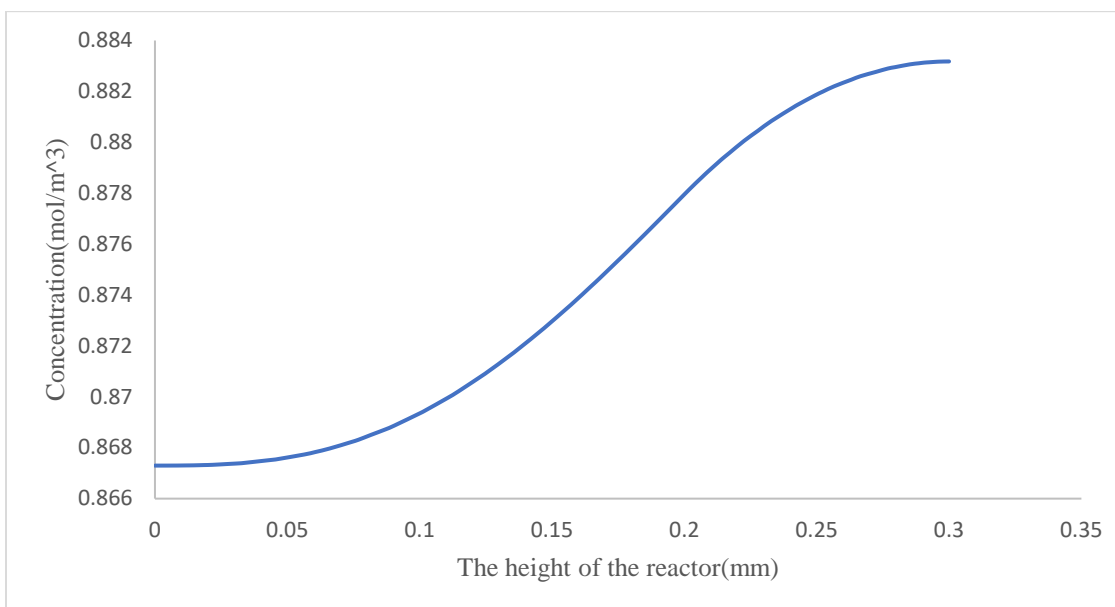


Figure 3.5 The concentration of phenol in the y-direction at x=5mm

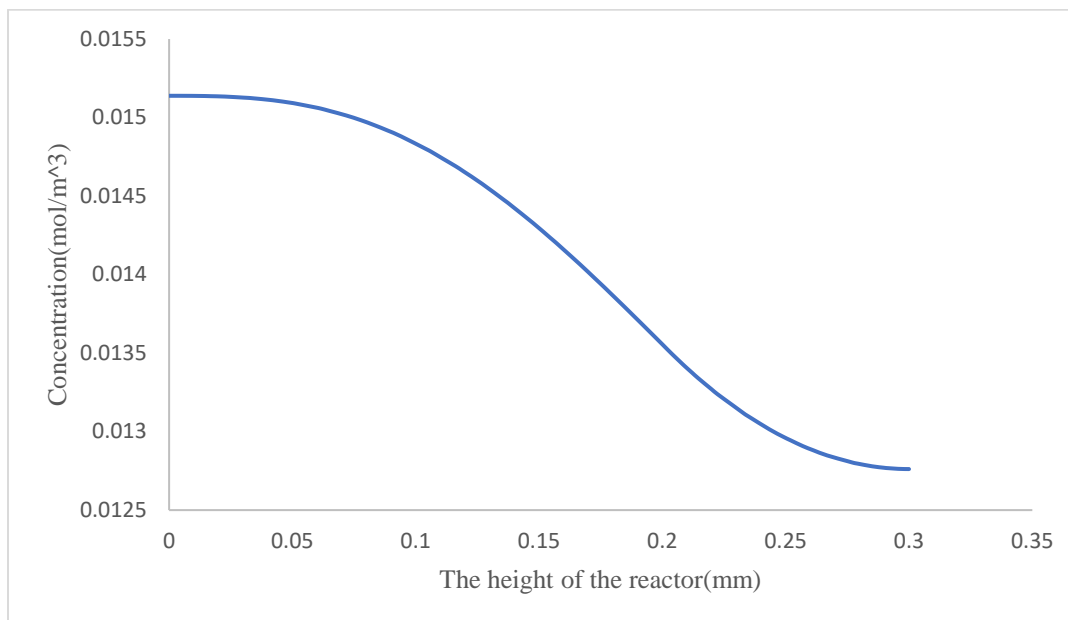


Figure 3.6 The concentration of p-chlorophenol in the y-direction at x=10mm

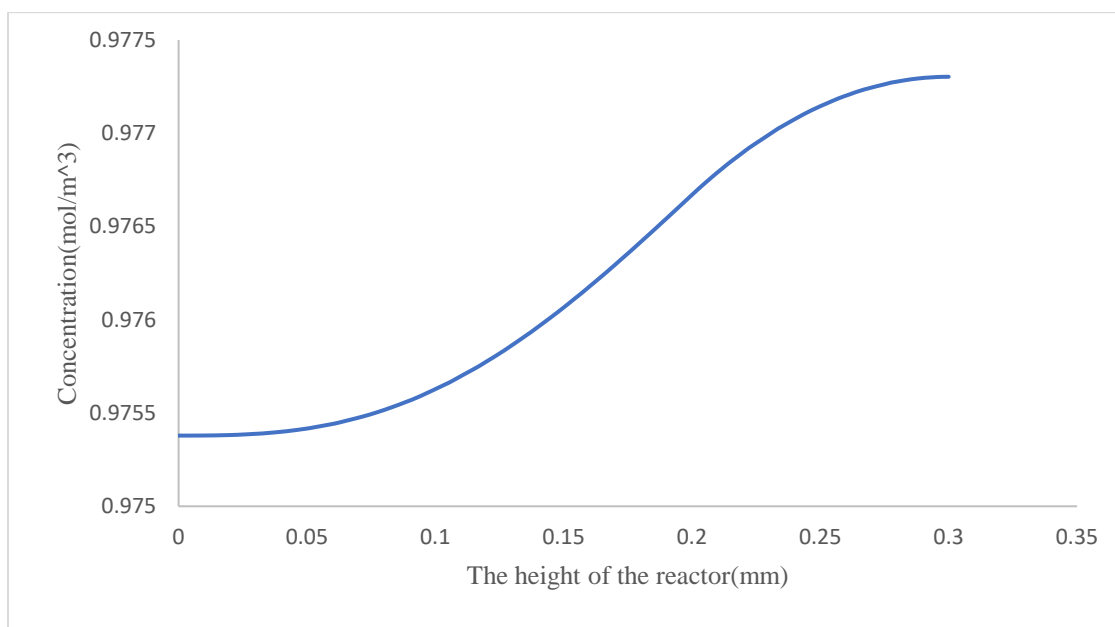


Figure 3.7 The concentration of phenol in the y-direction at x=10mm

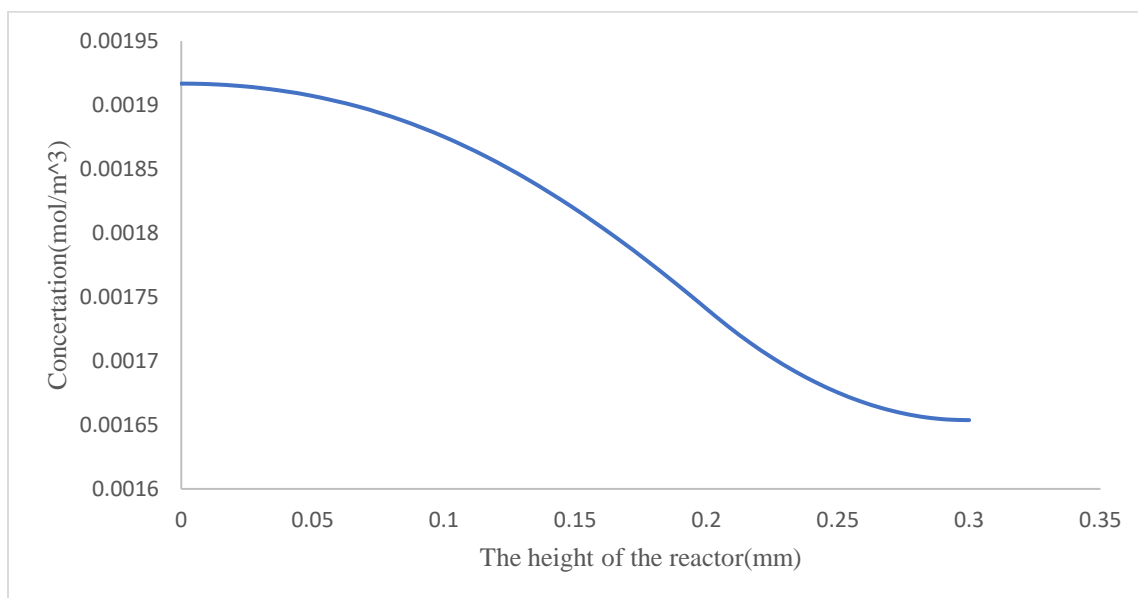


Figure 3.8 The concentration of p-chlorophenol in the y-direction at x=15mm

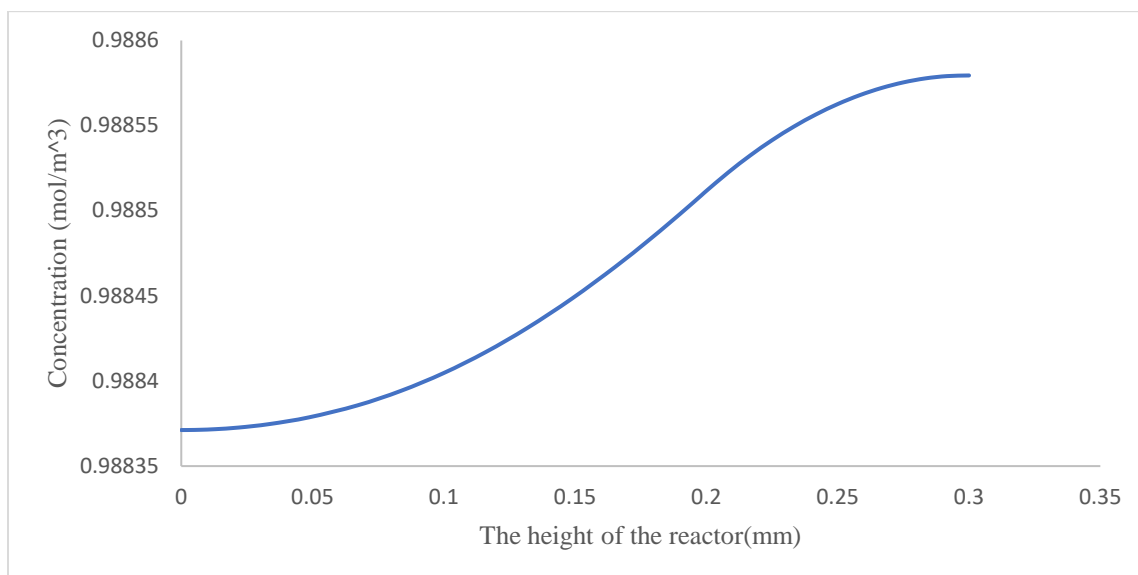


Figure 3.9 The concentration of phenol in the y-direction at x=15mm

When the reactant p-chlorophenol enters the gel phase, it begins to be adsorbed on the catalyst surface, and figure 3.10 shows the adsorption of p-chlorophenol. When the p-chlorophenol diffuses into the gel phase, the p-chlorophenol is consumed due to the adsorption of p-chlorophenol to the iron surface substrate and the direct adsorption to the palladium surface on the catalyst surface. The figure 3.10 shows the concentration of p-chlorophenol associated with iron surface $[R-Cl]^o$ increases and is followed by a decline because p-chlorophenol migrates from the iron surface to the palladium surface. The decrease of the slope of the curve means that the chemical kinetics of adsorption decreasing because of the concentration of $[R-Cl]^o$ reduces due to the migration. After the adsorption of the p-chlorophenol, the p-chlorophenol migrates from the iron surface to the palladium surface.

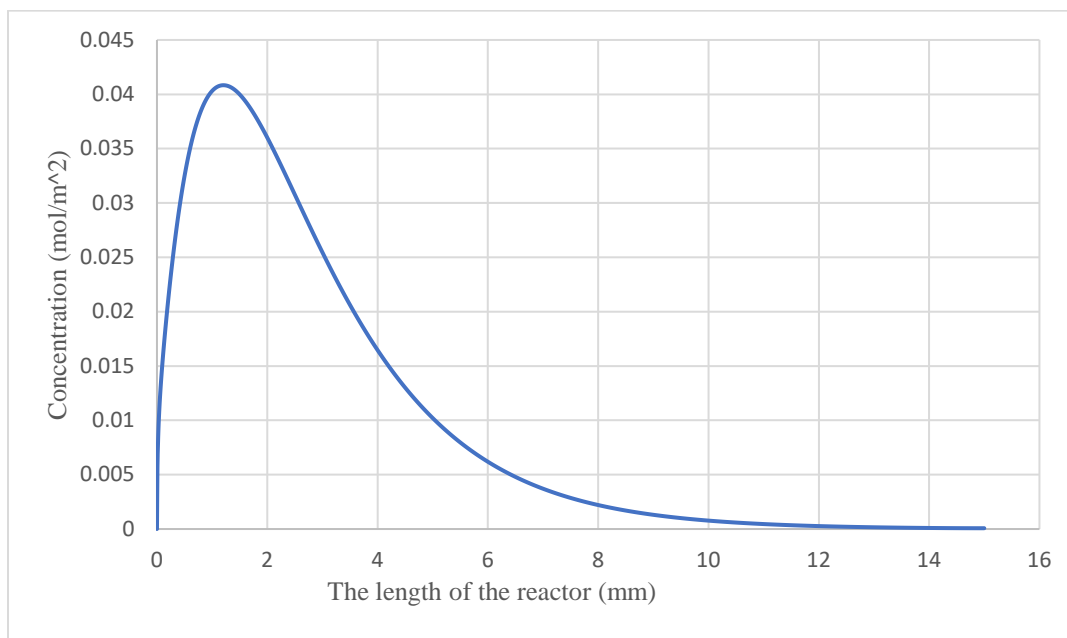


Figure 3.10 The concentration of p-chlorophenol on the iron surface

Figure 3.11 represents the concentration of p-chlorophenol on the palladium surface. Compared to the figure of $[R-Cl]^o$ with the figure of $[R-Cl]^*$, $[R-Cl]^*$ increases to the maximum and then decreases to zero. The production of $[R-Cl]^*$ can be explained by migration of $[R-Cl]^o$ from the iron surface to the palladium surface and the direct adsorption of p-chlorophenol from the liquid phase of the gel phase to the palladium surface. The consumption of $[R-Cl]^*$ is due to the first step of dechlorination. Since the total mass of p-chlorophenol in the fluid is minor, the p-chlorophenol on the palladium surface is consumed up by a large number of hydrogen radicals on the palladium surface.

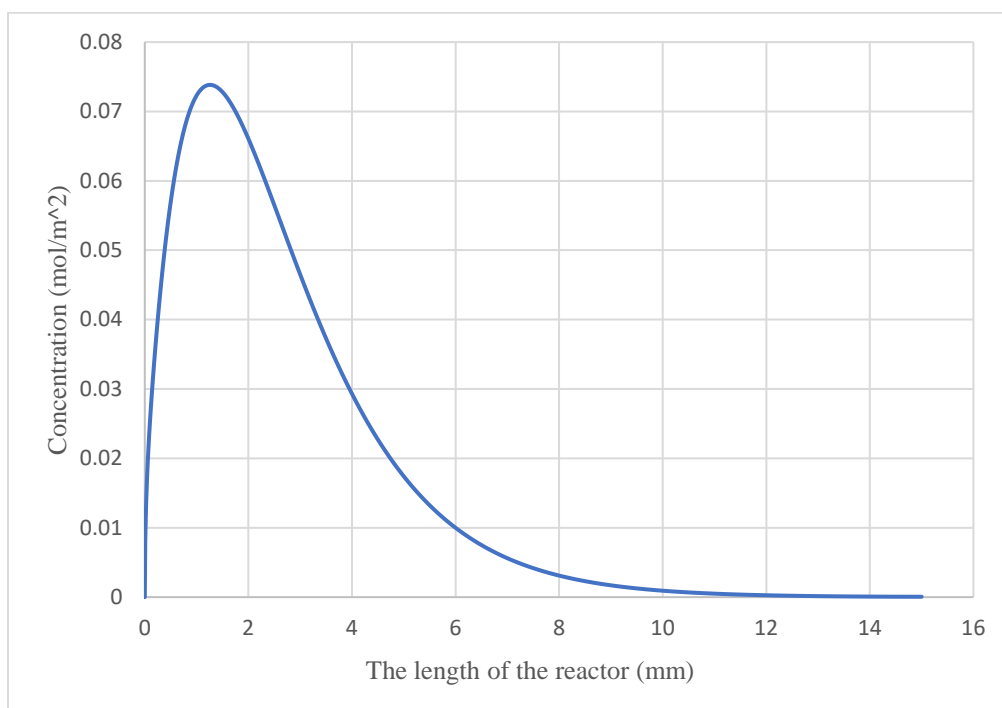


Figure 3.11 The concentration of p- chlorophenol on the palladium surface

At the same time, the hydrogen ions from the ionization of water molecules in the main fluid diffuse to the gel phase, they can be adsorbed on the iron surface and react with iron. Therefore, the concentration of hydrogen ions on the iron surface increases because of adsorption. When the hydrogen ions are accumulated around the iron surface, they can combine with the electrons on the iron surface to generate the hydrogen radicals. Figure 3.12 demonstrates that the concentration of hydrogen radicals on the iron surface increases because of the combination of hydrogen ions and electrons. These hydrogen radicals are so active that two of them produce one hydrogen molecules. Consequently, the concentration hydrogen radicals begin to decrease and end with zero.

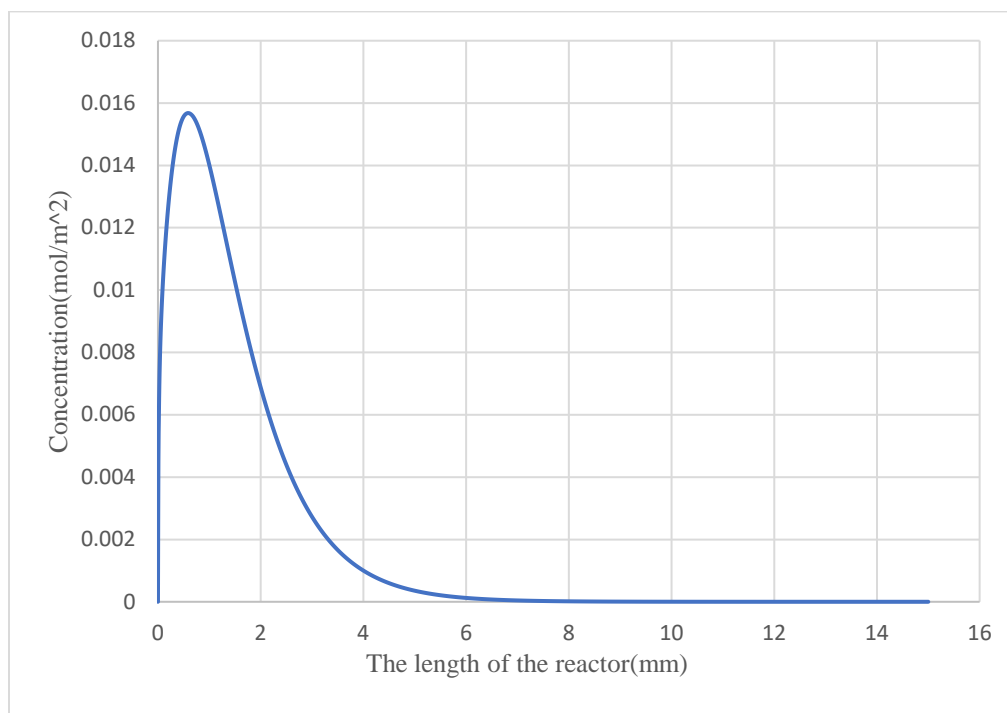


Figure 3.12 The concentration of hydrogen ions on the iron surface

The figure 3.14 shows the generation of hydrogen molecules on the iron surface, but the concentration of hydrogen molecules decrease since the hydrogen molecules on the iron surface can desorb from the iron surface to the liquid phase in the gel phase and migrate from the iron surface to palladium surface, as the figure 3.15 demonstrates. Additionally, figure 3.15 indicates that the amount of the hydrogen molecules that attached on the iron surface is comparatively lower than on the palladium surface since most of the hydrogen molecules accumulate around the palladium because palladium have well-behavior ability to adsorb hydrogen molecules due to its molecular space, which explains why the palladium can be served as the acceptable catalyst. The two figures prove that the use of palladium as the catalyst is a well-considered method. The hydrogen molecules reduce because they disassociate to the hydrogen radicals under the influence of palladium molecular.

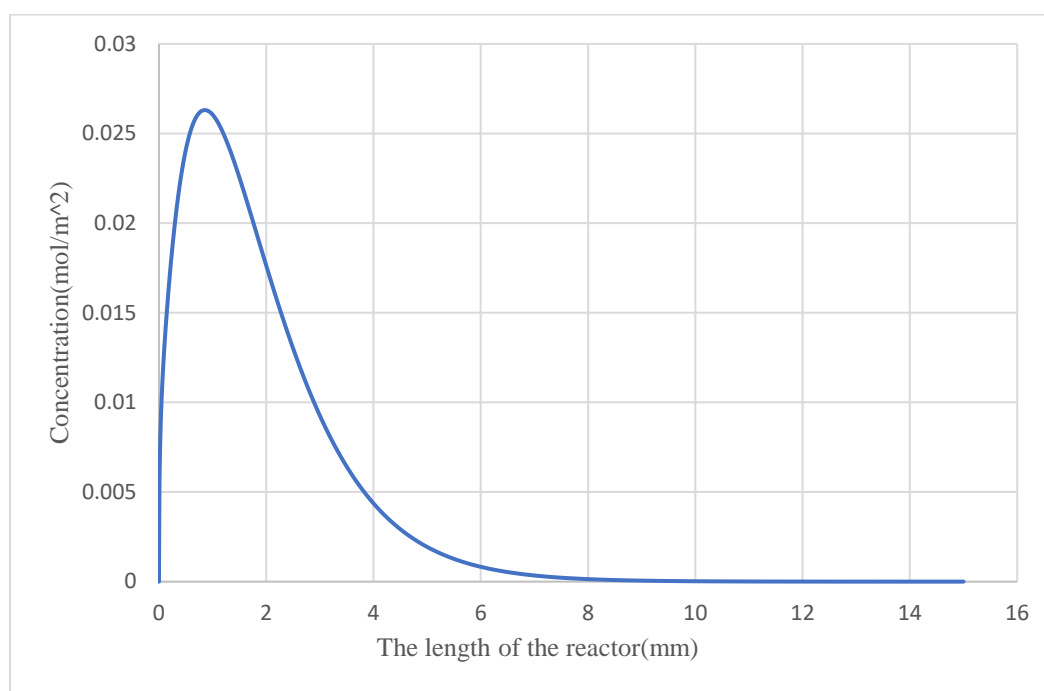


Figure 3.13 The concentration of hydrogen radicals on the iron surface

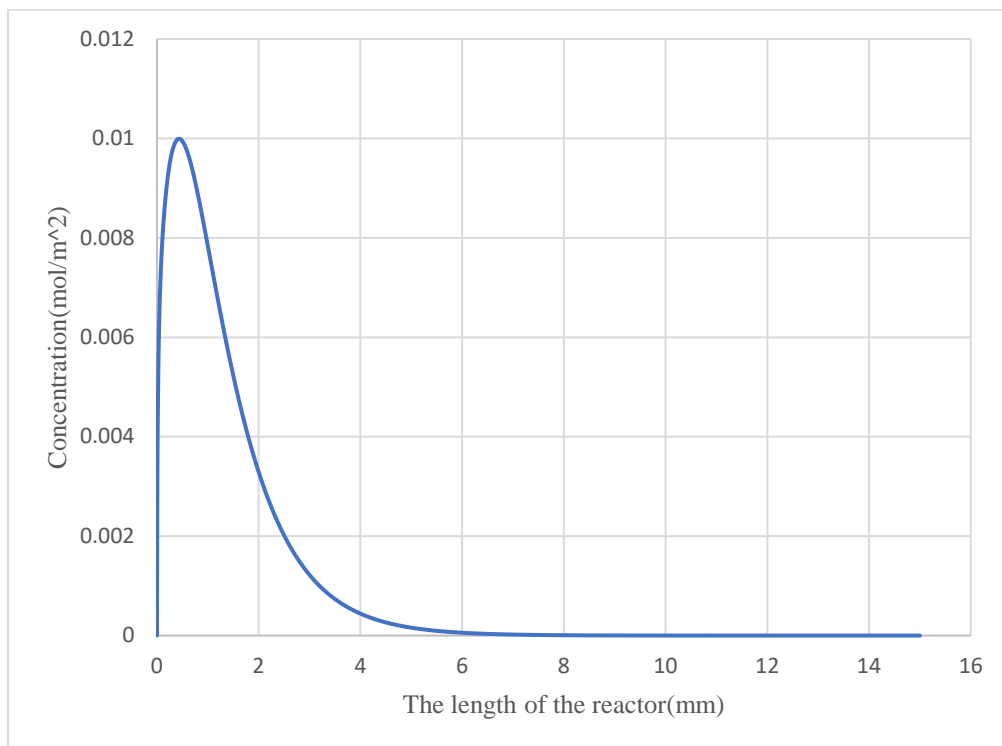


Figure 3.14 The concentration of hydrogen molecules on the iron surface

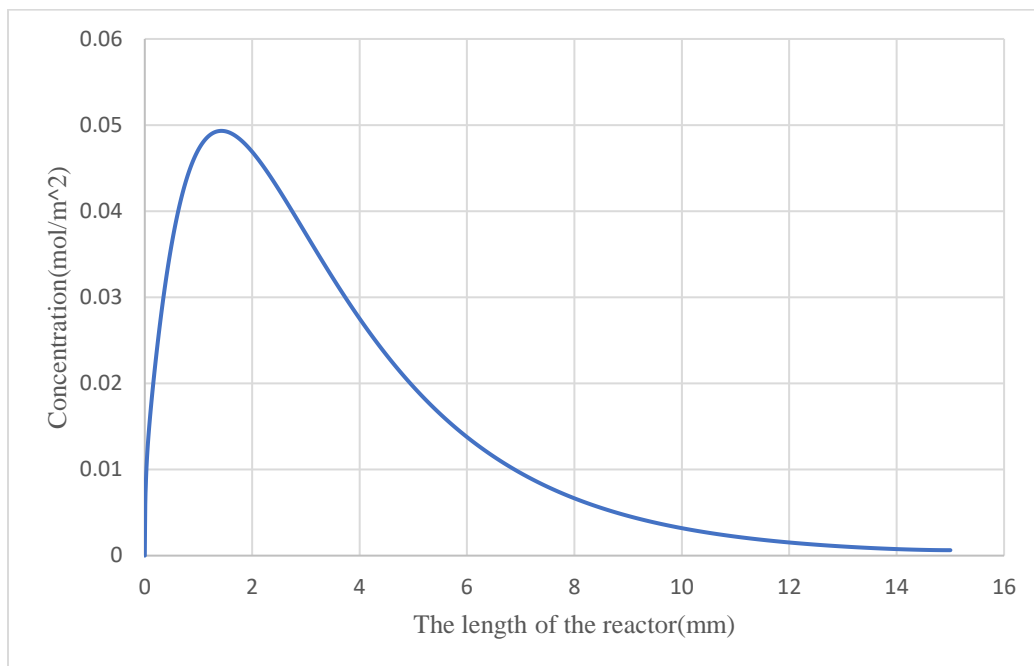


Figure 3.15 The concentration of hydrogen molecules on a palladium surface

The hydrogen molecules on the palladium surface can produce hydrogen radicals under the influence of palladium. The maximum number of hydrogen radicals are much than the number of hydrogen molecules on the palladium since one mole per unit surface area can create two moles radicals per unit surface area. Additionally, the size of radicals is much less, and they can occupy more surface area than the hydrogen molecules do. When the p-chlorophenol associated with palladium surface $[R-Cl]^*$ is created, the dechlorination begins. As if discussing previously, the dechlorination can be divided into two steps. Firstly, the intermediate products $[R-HCl]^*$ are produced. From the figure, the $[R-HCl]^*$ does not increase at the zero point, because the adsorption of p-chlorophenol onto the iron surface and direct adsorption of p-chlorophenol onto the palladium surface take time before the dechlorination occurs.

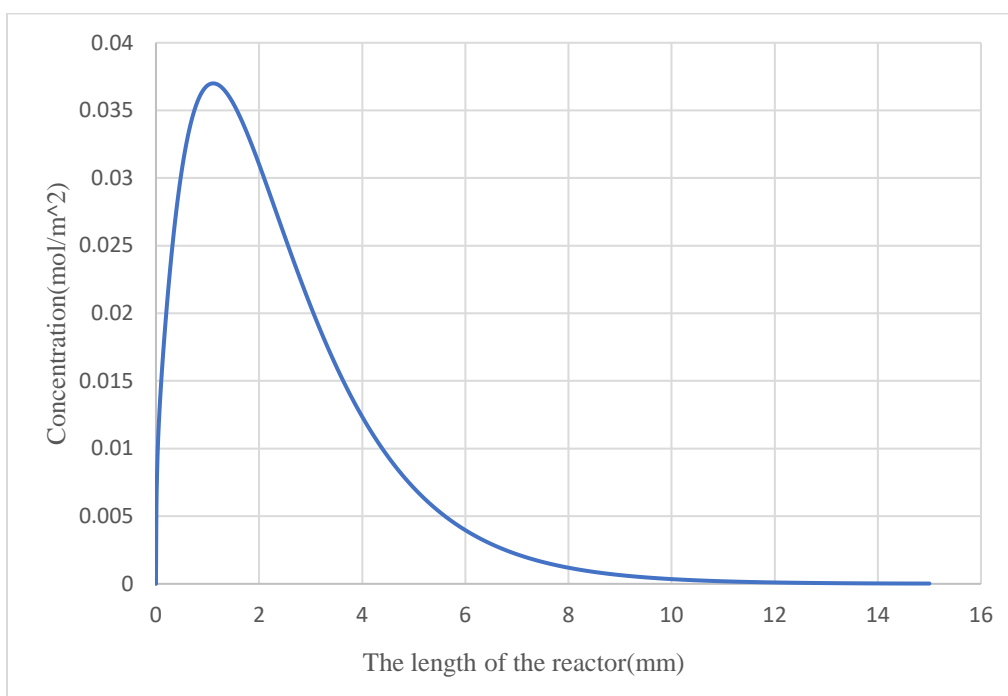


Figure 3.16 The concentration of hydrogen radicals on the palladium surface

When the final products phenol molecules associated with palladium surface $[R]^*$ generated, the phenol molecules desorb from the palladium surface to the gel phase. As a result, as the direct desorption proceeding, the concentration of $[R]_{gel}$ increases. However, with the decline of the concentration of $[R]^*$, the rate of desorption $[R]^*$ reduces as well, which cause the slope of the curve decreases. Finally, the concentration of phenol will stay constant when the dechlorination ends. Further, from figure 2.8, the phenol in the gel does not increase when the time is zero since a series of reactions happen such as adsorption, migration, and dechlorination before the direct desorption of $[R]^*$.

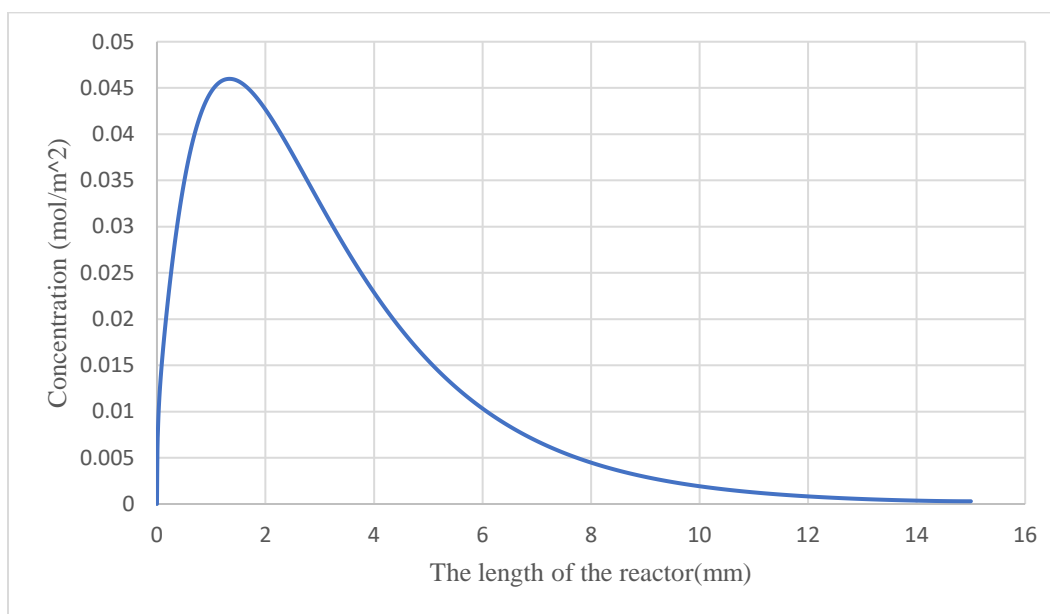


Figure 3.17 The figure for the concentration of intermediate products of dechlorination

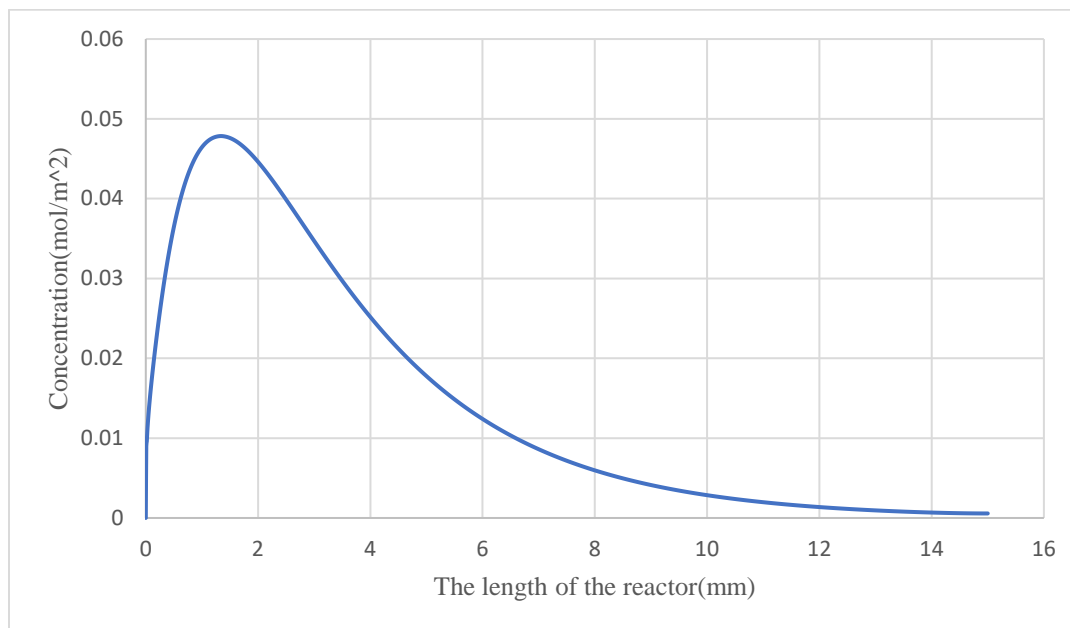


Figure 3.18 The concentration of phenol on the palladium surface

The iron surface iron substance can be occupied in the whole process; the inlet ratio of iron surface iron substance to the total catalyst surface is 0.9. Figure 3.19 shows the iron surface iron substance gradually decrease since the hydrogen radicals and p-chlorophenol molecules occupy them. However, most of the hydrogen radical and p-chlorophenol molecules desorb from the catalyst surface and migrate to the palladium surface. Therefore, some unoccupied iron surface iron substance can be created, which can be considered as the production of iron surface iron. The figure illustrates that the increasing trend of the iron surface iron substrate. Different from S^* / S S^o / S does not reduce to the zero, but it increases after a decrease, which can be explained by the desorption of p-chlorophenol molecules after adsorption of p-chlorophenol molecules. Therefore, S^o / S will increase when some of the occupied sites become unoccupied. Similarly, the final value of the S^o / S is equal to the inlet one since the total amount of reactants molecules occupying the iron surface is equal to the total amount of the molecules of the product leaving the iron surface.

The difference is that the S^o / S increases much more early than the S^* / S does, since desorption of molecules from iron surface to the gel phase occurs before the desorption of molecules from palladium surface to the gel phase.

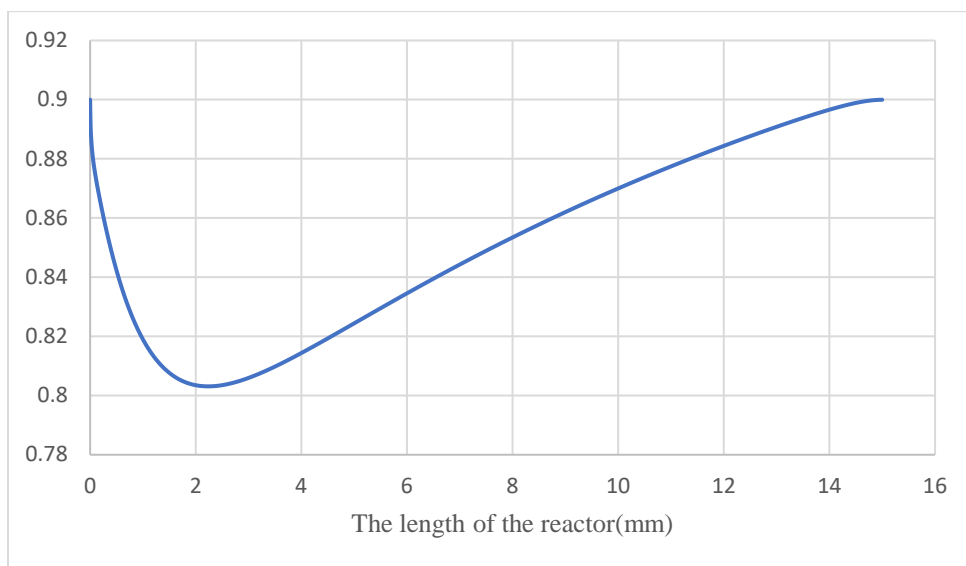


Figure 3.19 The concentration of iron surface

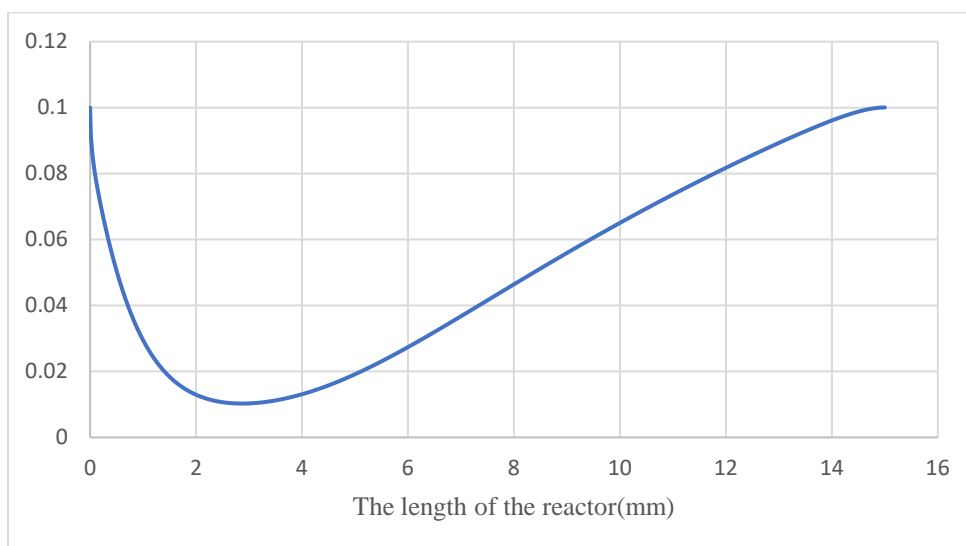


Figure 3.20 The concentration of palladium surface

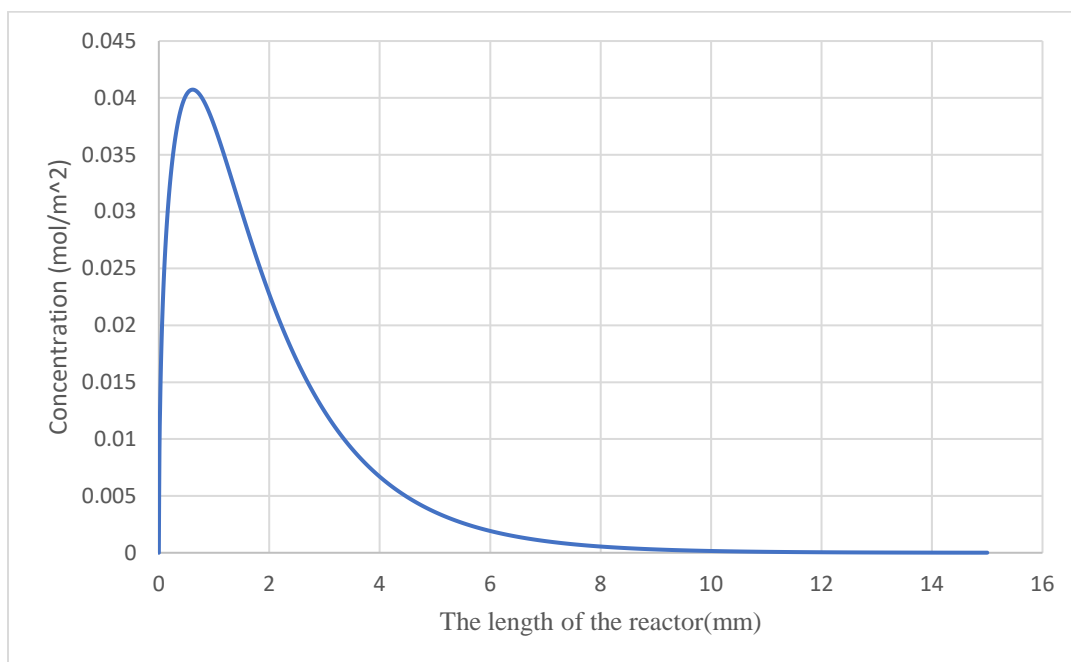


Figure 3.21 The concentration of electrons on the catalyst surface

Chapter 5 Conclusion

The proposed thesis contributes to science by creating a new method to dechlorinate p-chlorophenol with a solid catalyst based on microscale reactor. In the thesis, the mathematical model for the solid catalytic dechlorination reaction process will be developed. The mathematical model including the velocity of the profile of fluid, mass transfer of reactants and chemical kinetics for every species that is involved in the dechlorination occurring on the solid catalyst surface. The right mathematical model is helpful to understand the solid catalyzed reaction process. In addition, the thesis also covers how to design a microscale-based reactor to dechlorinate, which offer a creative way to clean up the waste in the environment. Based on the advantages of microscale-based reactors, they can contribute to eliminating the pollution deal with the polluted river. The Fe/Pd catalyst also has the potential to address the contaminated water issue efficiently. This way will be applied widespread due to their environmental-friendly characteristics and reasonable price. At last, the dechlorination by using microscale-based reactor will be performed in a lab. The experimental data will not only justify and validate the mathematical model but also test the performance of the creative microscale-based reactor. The valid and justified mathematical model will contribute to test the microscale-based reactors with various designs, the performance of the whole dechlorination process. The mathematical model also is likely to scale up version of the process and predict the final efficiency or production of the reaction under different reaction conditions.

Bibliography

B.G. Oliver, K.D. Nicol, Chlorobenzenes in sediments, water, and selected fish from Lakes Superior, Huron, Erie, and Ontario, *Environ. Sci. Technol.* 16 (1982) 532–536.

F. He, D.Y. Zhao, J.C. Liu, C.B. Roberts, Stabilization of Fe–Pd nanoparticles with sodium carboxymethyl cellulose for enhanced transport and dechlorination of trichloroethylene in soil and groundwater, *Ind. Eng. Chem. Res.* 46 (2007) 29–34.

Huang, Q., Liu, W., Peng, P., & Huang, W. (2013). Reductive dechlorination of tetrachlorobisphenol A by Pd/Fe bimetallic catalysts. *Journal of Hazardous Materials*, 262, 634–641.

Hessel, V. et al. (2013) Novel process windows for enabling, accelerating, and uplifting flow chemistry. *ChemSusChem* 6, 746–789

M. Ahmaruzzaman, Adsorption of phenolic compounds on low-cost adsorbents: a review, *Adv. Colloid Interf. Sci.* 143 (2004) 48–67.

H. Kim, H.J. Hong, Y.J. Lee, H.J. Shin, J.W. Yang, Degradation of trichloroethylene by iron surface iron immobilized in cationic exchange membrane, *Desalination* 223 (2008) 212–220.

R.P. Schwarzenbach, E. Molnar-Kubica, W. Giger, S.G. Wakeham, Distribution, residence time, and fluxes of tetrachloroethylene and 1,4-dichlorobenzene in Lake Zurich, Switzerland, *Environ. Sci. Technol.* 13 (1976) 1367–1373

Newman, S.G. and Jensen, K.F. (2013) The role of flow in green chemistry and engineering. *Green Chem.* 15, 1456–1472

W.S. Orth, R.W. Gillham, Dechlorination of trichloroethene in aqueous solution using Fe (0) *Environ. Sci. Technol.*, 30 (1996), pp. 66-71

Wohlgemuth, R., Plazl, I., Žnidaršič-Plazl, P., Gernaey, K. V., & Woodley, J. M. (2015). Microscale technology and biocatalytic processes: Opportunities and challenges for synthesis. *Trends in Biotechnology*, 33(5), 302-314.

W.A. Arnold, A.L. Roberts Pathways, and kinetics of chlorinated ethylene and chlorinated acetylene reaction with Fe (0) particles *Environ. Sci. Technol.*, 34 (2000), pp. 1794-1805

X.Y. Wang, C. Chen, H.L. Liu, J. Ma, Characterization and evaluation of catalytic dechlorination activity of Pd/Fe bimetallic nanoparticles, *Ind. Eng. Chem. Res.* 47 (2008) 8645–865

Yang, L, Zhang, S., Pan, B., & Zhang, W. (2011). Catalytic dechlorination of monochlorobenzene by Pd/Fe nanoparticles immobilized within a polymeric anion exchanger. *Chemical Engineering Journal*, 178, 161-167.

Zhang, X., Stefanick, S., & Villani, F. J. (2004). Application of Microreactor Technology in Process Development. *Organic Process Research & Development*, 8(3), 455-460.

Appendix A

Development of Navier-Stokes equation of p-chlorophenol in the main fluid

The velocity profile of p-chlorophenol can be expressed by the two equations in x and y-direction:

$$\text{X-direction: } \rho \left[\frac{\partial u_x}{\partial t} + u_x \frac{\partial u_x}{\partial x} + u_y \frac{\partial u_x}{\partial y} \right] = -\frac{\partial P}{\partial x} + \mu \left[\frac{\partial^2 u_x}{\partial x^2} + \frac{\partial^2 u_x}{\partial y^2} \right] + \rho g_x$$

$$\text{Y-direction: } \rho \left[\frac{\partial u_y}{\partial t} + u_x \frac{\partial u_y}{\partial x} + u_y \frac{\partial u_y}{\partial y} + u_z \frac{\partial u_y}{\partial z} \right] = -\frac{\partial P}{\partial y} + \mu \left[\frac{\partial^2 u_y}{\partial x^2} + \frac{\partial^2 u_y}{\partial y^2} \right] + \rho g_y$$

There is no velocity of p-chlorophenol along the y-direction, so the whole Navier Stokes equation for Y direction can be canceled. Consequently, there is only velocity profile of p-chlorophenol along the x-direction left

After canceling the equation for y-direction simplified the equation for x-direction is necessary.

Since the whole process previous is assumed as steady state, the term $\frac{\partial u_x}{\partial t}$ related to the time

can be eliminated:

$$\rho \left[u_x \frac{\partial u_x}{\partial x} \right] = -\frac{\partial p}{\partial x} + \mu \left[\frac{\partial^2 u_x}{\partial x^2} + \frac{\partial^2 u_x}{\partial y^2} \right] + \rho g_x$$

The term g_x can be eliminated because there is no gravitation along the x-direction and the equation can be further simplified:

$$\rho \left(u_x \frac{\partial u_x}{\partial x} \right) = -\frac{\partial p}{\partial x} + \mu \left[\frac{\partial^2 u_x}{\partial x^2} + \frac{\partial^2 u_x}{\partial y^2} \right]$$

Based on the previous assumption, the velocity of p-chlorophenol along x-direction is constant.

Therefore, the term $u_x \frac{\partial u_x}{\partial x} = 0$ can be eliminated, so the final simplified equation can be

obtained:

$$\boxed{\frac{\partial P}{\partial x} = \mu \left(\frac{\partial^2 u_x}{\partial y^2} \right)}$$

Appendix B

Development of mass balance equations for p-chlorophenol in the main fluid

The mathematical model of p-chlorophenol mass transfer in the microscale-based reactor can be developed separately in main fluid and in gel part. The general mass transfer of p-chlorophenol can be expressed by the equation: Input-Output-Generation=Accumulation.

$$\text{The Input } u_x C_{[R-Cl]_{Fluid}} \Big|_x - D_1 \frac{\partial C_{[R-Cl]_{Fluid}}}{\partial x} \Big|_x - D_1 \frac{\partial C_{[R-Cl]_{Fluid}}}{\partial y} \Big|_y$$

$$\text{Output: } u_x C_{[R-Cl]_{Fluid}} \Big|_{x+\Delta x} - D_2 \frac{\partial C_{[R-Cl]_{Fluid}}}{\partial x} \Big|_{x+\Delta x} - D_2 \frac{\partial C_{[R-Cl]_{Fluid}}}{\partial y} \Big|_{y+\Delta y}$$

Assume the p-chlorophenol only diffuses in x and y-direction, the terms that are related to the z-direction can be eliminated. The mass conservation equation for p-chlorophenol in the gel phase can be developed:

$$D_1 \left[\frac{\partial^2 C_{[R-Cl]_{Fluid}}}{\partial x^2} + \frac{\partial^2 C_{[R-Cl]_{Fluid}}}{\partial y^2} \right] - u_x \left[\frac{\partial C_{[R-Cl]_{Fluid}}}{\partial x} + \frac{\partial C_{[R-Cl]_{Fluid}}}{\partial y} \right] - r_{[R-Cl]_{Fluid}} = \frac{\partial C_{[R-Cl]_{Fluid}}}{\partial t}$$

Since there is no reaction in the main fluid, so no generation occurs and the term $r_{[C_{R-Cl}]_{Fluid}}$ can be canceled:

$$D_1 \left[\frac{\partial^2 C_{[R-Cl]_{Fluid}}}{\partial x^2} + \frac{\partial^2 C_{[R-Cl]_{Fluid}}}{\partial y^2} \right] - u_x \left[\frac{\partial C_{[R-Cl]_{Fluid}}}{\partial x} + \frac{\partial C_{[R-Cl]_{Fluid}}}{\partial y} \right] = \frac{\partial C_{[R-Cl]_{Fluid}}}{\partial t}$$

Assume the flow of p-chlorophenol in main fluid part is in the steady state, the term $\frac{\partial C_{[R-Cl]_{Fluid}}}{\partial t}$

can be eliminated:

$$D_1 \left[\frac{\partial^2 C_{[R-Cl]_{Fluid}}}{\partial x^2} + \frac{\partial^2 C_{[R-Cl]_{Fluid}}}{\partial y^2} \right] - u_x \left[\frac{\partial C_{[R-Cl]_{Fluid}}}{\partial x} + \frac{\partial C_{[R-Cl]_{Fluid}}}{\partial y} \right] = 0$$

Assume the velocity of p-chlorophenol is only along the x-direction, so the term $\frac{\partial C_{[R-Cl]_{Fluid}}}{\partial y}$ can

be eliminated. The final simplified equation for mass transfer of p-chlorophenol in the main fluid can be obtained:

$$D_1 \left[\frac{\partial^2 C_{[R-Cl]_{Fluid}}}{\partial x^2} + \frac{\partial^2 C_{[R-Cl]_{Fluid}}}{\partial y^2} \right] - u_x \left[\frac{\partial C_{[R-Cl]_{Fluid}}}{\partial x} \right] = 0$$

However, the generation is not equal to zero in the catalyst part because a lot of reaction occurring in there. Since the mass transfer is related to the volumetric p-chlorophenol in the reactor, the generation of p-chlorophenol in mass transfer should be concerned with consumption and production of p-chlorophenol in the gel phase rather than solid catalyst surface, which includes adsorption of p-chlorophenol, direct adsorption of p-chlorophenol and the desorption of p-chlorophenol. Therefore, the total generation can be expressed as:

$$r_{[R-Cl]_{gel}} = -r_{[R-Cl]_{gel} \rightarrow [R-Cl]^o} - r_{[R-Cl]_{gel} \rightarrow [R-Cl]^*} + r_{[R-Cl]^o \rightarrow [R-Cl]_{gel}}$$

There is no velocity of p-chlorophenol in catalyst part, so the terms that are related to the convection can be eliminated:

$$D_2 \left[\frac{\partial^2 [C_{R-Cl}]_{gel}}{\partial x^2} + \frac{\partial^2 [C_{R-Cl}]_{gel}}{\partial y^2} + \frac{\partial^2 [C_{R-Cl}]_{gel}}{\partial z^2} \right] - r_{[R-Cl]_{gel}} = \frac{\partial [C_{R-Cl}]_{gel}}{\partial t}$$

Plugging in the net chemical kinetics of p-chlorophenol in the liquid or gel phase, the final equation for mass transfer of p-chlorophenol can be expressed :

$$D_2 \left[\frac{\partial^2 [C_{R-Cl}]_{gel}}{\partial x^2} + \frac{\partial^2 [C_{R-Cl}]_{gel}}{\partial y^2} \right] - r_{[R-Cl]_{gel} \rightarrow [R-Cl]^o} - r_{[R-Cl]_{gel} \rightarrow [R-Cl]^*} = 0$$

Appendix C

Values of parameters in the COMSOL software

L	The length of the microscale based reactor	15 [mm]
d_1	The height of the gel phase	0.1 [mm]
d_2	The height of the main fluid	0.2 [mm]
$\frac{S^o}{S}$	The inlet concentration of the catalyst surface containing surface of the iron surface	$0.9 \left[\frac{m_{s^o}^2}{m_c^2} \right]$
$\frac{S^*}{S}$	The initial concentration of the catalyst surface containing palladium surface	$0.1 \left[\frac{m_{s^*}^2}{m_c^2} \right]$
$\frac{S}{V}$	The total surface area of catalyst per volume of the microscale-based scale reactor	$10 \left[\frac{m_c^2}{m_r^3} \right]$
$\frac{V}{S}$	The volume of the microscale-based scale reactor per total surface area of the catalyst	$0.1 \left[\frac{m_r^3}{m_c^2} \right]$
$C_{[R-Cl]inlet}$	The inlet concentration of p-chlorophenol at the entrance of the reactor	$1 \left[\frac{mol}{m^3} \right]$
$C_{[H^+]_{gel}}$	The inlet volumetric concentration of hydrogen radicals in the gel phase	$1 \times 10^{-4} \left[\frac{mol [H^+]_{gel}}{m_g^3} \right]$
D_1	The diffusion coefficient in the main fluid	$8.6 \times 10^{-9} \left[\frac{m^2}{s} \right]$

D_2	The diffusion coefficient in the liquid phase of the gel phase	$8 \times 10^{-10} \left[\frac{m^2}{s} \right]$
k_8	The rate constant of adsorption of hydrogen ions on the iron surface substrate	$1 \left[\frac{m_c^2}{m_{s^o}^2 \cdot s} \right]$
k_{10}	The rate constant of adsorption of hydrogen ions on the palladium surface	$2 \left[\frac{m_c^2}{m_{s^*}^2 \cdot s} \right]$
k_{11}	The rate constant of production of hydrogen radicals on the palladium surface	$0.0002 \left[\frac{1}{s} \right]$
k_{13}	The rate constant of production of hydrogen molecules on the iron surface	$0.001 \left[\frac{m_c^2}{m_{s^o}^2 \cdot s} \right]$
k_{14}	The rate constant of migration of hydrogen molecules from the iron surface to palladium surface	$0.125 \left[\frac{m_c^2}{m_{s^*}^2 \cdot s} \right]$
k_{18}	The rate constant of disassociation of hydrogen molecules associated with palladium surface	$1 \left[\frac{1}{s} \right]$
k_{19}	The rate constant of adsorption of p-chlorophenol molecules to the iron surface substrate	$0.009 \left[\frac{m_c^2}{m_{s^o}^2 \cdot s} \right]$
k_{22}	The rate constant of direct absorption of p-chlorophenol to palladium surface	$0.04 \left[\frac{m_c^2}{m_{s^*}^2 \cdot s} \right]$
k_{21}	The rate constant of migration of p-chlorophenol molecules from the iron surface substrate to palladium surface	$0.12 \left[\frac{m_s^2}{m_{s^*}^2 \cdot s} \right]$
k_{23}	The rate constant of first-step disassociation of p-chlorophenol on the palladium surface	$0.001 \left[\frac{m_c^2}{mol [H_R]^* \cdot s} \right]$

k_{24}	The rate constant of second-step disassociation of p-chlorophenol on the palladium surface	$0.37 \left[\frac{m_c^2}{\text{mol}[H_R]^* \cdot s} \right]$
k_{25}	The rate constant of direct desorption of phenol from palladium surface to gel phase	$0.015 \left[\frac{1}{s} \right]$
$\xi_{[H_2]^o \rightarrow [H_2]^*}$	The stoichiometric conversion factor	$1 \left[\text{mol}[H_2]^* / \text{mol}[H_2]^o \right]$
$\xi_{[H_2]^* \rightarrow [H_R]^*}$	The stoichiometric conversion factor	$1 \left[\text{mol}[H_R]^* / \text{mol}[H_2]^* \right]$
$\xi_{[R-Cl]_{gel} \rightarrow [R-Cl]^o}$	The stoichiometric conversion factor	$1 \left[\text{mol}[R-Cl]^o / \text{mol}[R-Cl] \right]$
$\xi_{[R-Cl]^o \rightarrow [R-Cl]^*}$	The stoichiometric conversion factor	$1 \left[\text{mol}[R-Cl]^* / \text{mol}[R-Cl]^o \right]$
$\xi_{[R-Cl]_{gel} \rightarrow [R-Cl]^*}$	The stoichiometric conversion factor	$1 \left[\text{mol}[R-Cl]^* / \text{mol}[R-Cl] \right]$
$\xi_{[R-Cl]^* \rightarrow [R-HCl]^*}$	The stoichiometric conversion factor	$1 \left[\text{mol}[R-HCl]^* / \text{mol}[R-Cl]^* \right]$
$\xi_{[R-HCl]^* \rightarrow [R]^*}$	The stoichiometric conversion factor	$1 \left[\text{mol}[R]^* / \text{mol}[R-HCl]^* \right]$
$\eta_{S^o[H_2]^o}$	Constant relating to the surface of the iron surface substrate S^o that is occupied with one mole of $[H_2]$.	$2 \times 10^4 \left[m_{S^o}^2 / \text{mol}[H_2]^o \right]$
$\eta_{S^o[H^+]^o}$	Constant relating to the surface of the iron surface substrate S^o that is occupied with one mole of $[H^+]$.	$2 \times 10^4 \left[m_{S^o}^2 / \text{mol}[H_2]^o \right]$

$\eta_{S^o[R-Cl]^o}$	Constant relating to the surface of the iron surface substrate S^o that is occupied with one mole of $[R-Cl]$.	$3 \times 10^4 \left[m^2_{S^o} / mol [R-Cl]^o \right]$
$\eta_{S^*[R-Cl]^*}$	Constant relating the surface of palladium surface S^* that is occupied with one mole of $[R-Cl]$.	$3 \times 10^4 \left[m^2_{S^*} / mol [R-Cl]^* \right]$
$\eta_{S^*[H_2]^*}$	Constant relating the surface of palladium surface S^* that is occupied with one mole of $[H_2]$.	$2 \times 10^4 \left[m^2_{S^*} / mol [H_2]^* \right]$
$\eta_{S^*[R]^*}$	Constant relating the surface of palladium surface S^* that is occupied with one mole of $[R]$.	$2.5 \times 10^4 \left[m^2_{S^*} / mol [R]^* \right]$

Appendix D

Development of mass balance equations of species on the catalyst surface

Mass balance equations for hydrogen ions on the iron surface $[H_2]^o$:

The hydrogen molecules in the gel phase can be adsorbed by the iron surface substrate, but the Palladium metal adsorbs most of them because the ability of the Palladium metal is super higher than the iron surface substrate. Since the net chemical kinetics for $[H_2]^o$ is expressed and there is no diffusion of $[H_2]^o$ the final mass transfer equation for $[H_2]^o$ can be expressed:

$$\cancel{D_2 \frac{\partial^2 C_{[H_2]^o}}{\partial x^2}} + \cancel{D_2 \frac{\partial^2 C_{[H_2]^o}}{\partial y^2}} + \Delta r_{[H_2]^o} = \frac{dC_{[H_2]^o}}{dt}$$

$$k_{13} \cdot C_{[H_R]^o} \cdot C_{[H_R]^o} \cdot \xi_{[H_R]^o \rightarrow [H_2]^o} - k_{15} \cdot C_{[H_2]^o} \cdot \xi_{[H_2]^o \rightarrow [H_2]_{gel}} \cdot \frac{S}{V_g} - k_{14} \cdot C_{[H_2]^o} \cdot \frac{S^*}{S} = \frac{dC_{[H_2]^o}}{dt}$$

Mass balance equations for hydrogen molecules on the palladium surface $[H_2]^*$:

When the hydrogen molecules arrive at the palladium metal, they can be dissociated to two hydrogen radicals, under the influence of palladium metal. Since the net chemical kinetics for $[H_2]^*$ is expressed and there is no diffusion of $[H_2]^*$ the final mass transfer equation for $[H_2]^*$ can be expressed:

$$\cancel{D_2 \frac{\partial^2 C_{[H_2]^*}}{\partial x^2}} + \cancel{D_2 \frac{\partial^2 C_{[H_2]^*}}{\partial y^2}} + \Delta r_{[H_2]^*} = 0$$

$$k_{14} \cdot C_{[H_2]^o} \cdot \frac{S^*}{S} \cdot \xi_{[H_2]^o \rightarrow [H_2]^*} + k_{17} \cdot C_{[H_2]_{gel}} \cdot \frac{S^*}{S} \cdot \xi_{[H_2]_{gel} \rightarrow [H_2]^*} \cdot \frac{V_g}{S} - k_{18} \cdot C_{[H_2]^*} \cdot \frac{S^*}{S} = 0$$

Mass balance equations for hydrogen radicals on the palladium surface $[H_R]^*$:

As the essential reactants of the dechlorination, hydrogen radicals are almost entirely consumed at the palladium surface. Since the net chemical kinetics for $[H_R]^*$ is expressed and there is no diffusion of $[H_R]^*$, the final mass transfer equation for $[H_R]^*$ can be expressed:

$$\cancel{D_2 \frac{\partial^2 C_{[H_R]^*}}{\partial x^2}} + \cancel{D_2 \frac{\partial^2 C_{[H_R]^*}}{\partial y^2}} + \Delta r_{[H_R]^*} = 0$$

$$k_{11} \cdot C_{[H^+]^*} \cdot \xi_{[H^+]^* \rightarrow [H_R]^*} + k_{18} \cdot C_{[H_2]^*} \cdot \frac{S^*}{S} \cdot \xi_{[H_2]^* \rightarrow [H_R]^*} - k_{23} \cdot C_{[R-Cl]^*} \cdot C_{[H_R]^*} - k_{24} \cdot C_{[R-HCl]^*} \cdot C_{[H_R]^*} = 0$$

Mass balance equations for p-chlorophenol on the iron surface $[R-Cl]^o$:

The p-chlorophenol molecules in the gel phase are adsorbed by the iron surface substrate, forming $[R-Cl]^o$. Since the net chemical kinetics for $[R-Cl]^o$ is expressed and there is no diffusion of $[R-Cl]^o$, the final mass transfer equation for $[R-Cl]^o$ can be expressed:

$$\cancel{D_2 \frac{\partial^2 C_{[R-Cl]^o}}{\partial x^2}} + \cancel{D_2 \frac{\partial^2 C_{[R-Cl]^o}}{\partial y^2}} + \Delta r_{[R-Cl]^o} = 0$$

$$k_{19} \cdot C_{[R-Cl]^o} \cdot \frac{S^o}{S} \cdot \xi_{R-Cl \rightarrow [R-Cl]^o} \cdot \frac{V_g}{S} - k_{21} \cdot C_{[R-Cl]^o} \cdot \frac{S^*}{S} - k_{20} \cdot C_{[R-Cl]^o} = 0$$

Mass balance equations for p-chlorophenol on the palladium surface $[R-Cl]^*$:

Some of p-chlorophenol in the gel phase can be directly adsorbed to the palladium surface, and p-chlorophenol molecules on the iron surface substrate migrate to the palladium surface. Since the

net chemical kinetics for $[R-Cl]^*$ is expressed and there is no diffusion of $[R-Cl]^*$, the final mass transfer equation for $[R-Cl]^*$ can be expressed:

$$\cancel{D_2 \frac{\partial^2 C_{[R-Cl]^*}}{\partial x^2}} + \cancel{D_2 \frac{\partial^2 C_{[R-Cl]^*}}{\partial y^2}} + \Delta r_{[R-Cl]^*} = 0$$

$$k_{21} \cdot C_{[R-Cl]^o} \cdot \frac{S^*}{S} \cdot \xi_{[R-Cl]^o \rightarrow [R-Cl]^*} + k_{22} \cdot C_{[R-Cl]_{gel}} \cdot \frac{S^*}{S} \cdot \xi_{[R-Cl]_{gel} \rightarrow [R-Cl]^*} \cdot \frac{V_g}{S} - k_{23} \cdot C_{[R-Cl]^*} \cdot C_{[H_R]^*} = 0$$

Mass balance equations for intermediate species on the palladium surface $[R-HCl]^*$:

The dechlorination has been investigated in the previous chapter; the intermediate species $[R-HCl]^*$ is generated in the first step of dechlorination. Since the net chemical kinetics for $[R-HCl]^*$ is expressed and there is no diffusion of $[R-HCl]^*$, the final mass transfer equation for $[R-HCl]^*$ can be expressed:

$$\cancel{D_2 \frac{\partial^2 C_{[R-HCl]^*}}{\partial x^2}} + \cancel{D_2 \frac{\partial^2 C_{[R-HCl]^*}}{\partial y^2}} + \Delta r_{[R-HCl]^*} = 0$$

$$k_{23} \cdot C_{[R-Cl]^*} \cdot C_{[H_R]^*} \cdot \xi_{[R-Cl]^* \rightarrow [R-HCl]^*} - k_{24} \cdot C_{[R-HCl]^*} \cdot C_{[H_R]^*} = 0$$

Mass balance equations for phenol on the palladium surface $[R]^*$:

The final products generate around the palladium surface. The process of developing mass transfer equation for $[R]^*$ is explored in the Appendix L. Since the net chemical kinetics for $[R]^*$

is expressed and there is no diffusion of $[R]^*$, the final mass transfer equation for $[R]^*$ can be represented:

$$\cancel{D_2 \frac{\partial^2 C_{[R]^*}}{\partial x^2}} + \cancel{D_2 \frac{\partial^2 C_{[R]^*}}{\partial y^2}} + \Delta r_{[R]^*} = \frac{dC_{[R]^*}}{dt}$$

$$k_{24} \cdot C_{[R-HCl]^*} \cdot C_{[H_R]^*} \cdot \xi_{[R-HCl]^* \rightarrow [R]^*} - k_{25} \cdot C_{[R]^*} = \frac{dC_{[R]^*}}{dt}$$

Appendix E

The screen image of the numerical model built in COMSOL software

